Quaternary Science Reviews 307 (2023) 108055

Contents lists available at ScienceDirect

Quaternary Science Reviews

journal homepage: www.elsevier.com/locate/quascirev

Holocene vegetation dynamics of circum-Arctic permafrost peatlands

Richard E. Fewster [a, *], Paul J. Morris [a], Graeme T. Swindles [b, c], Ruza F. Ivanovic [d], Claire C. Treat [e], Miriam C. Jones [f]

[a] School of Geography, University of Leeds, Leeds, LS2 9JT, United Kingdom
[b] Geography, School of Natural and Built Environment, Queen's University Belfast, Belfast, BT7 1NN, United Kingdom
[c] Ottawa-Carleton Geoscience Centre and Department of Earth Sciences, Carleton University, Ottawa, Ontario, Canada
[d] School of Earth and Environment, University of Leeds, Leeds, LS2 9JT, United Kingdom
[e] Alfred Wegener Institute Helmholtz Center for Polar and Marine Research, Potsdam, Germany
[f] Florence Bascom Geoscience Center, U.S. Geological Survey, Reston, USA

ARTICLE INFO

Article history:
Received 5 December 2022
Received in revised form
24 February 2023
Accepted 18 March 2023
Available online xxx

Handling Editor: Yan Zhao

Keywords:
Permafrost
Peatlands
Plant macrofossils
Shrubification
Vegetation dynamics
Palaeoecology
Holocene
Paleogeography

ABSTRACT

Vegetation shifts in circum-Arctic permafrost peatlands drive feedbacks with important consequences for peatland carbon budgets and the extent of permafrost thaw under changing climate. Recent shrub expansion across Arctic tundra environments has led to an increase in above-ground biomass, but the long-term spatiotemporal dynamics of shrub and tree growth in circum-Arctic peatlands remain unquantified. We investigate changes in peatland vegetation composition during the Holocene using previously-published plant macrofossil records from 76 sites across the circum-Arctic permafrost zone. In particular, we assess evidence for peatland shrubification at the continental scale. We identify increasing abundance of woody vegetation in circum-Arctic peatlands from ~8000 years BP to present, coinciding with declining herbaceous vegetation and widespread *Sphagnum* expansion. Ecosystem shifts varied between regions and present-day permafrost zones, with late-Holocene shrubification most pronounced where permafrost coverage is presently discontinuous and sporadic. After ~600 years BP, we find a proliferation of non-*Sphagnum* mosses in Fennoscandia and across the present-day continuous permafrost zone; and rapid expansion of *Sphagnum* in regions of discontinuous and isolated permafrost as expected following widespread fen-bog succession, which coincided with declining woody vegetation in eastern and western Canada. Since ~200 years BP, both shrub expansion and decline were identified at different sites across the pan-Arctic, highlighting the complex ecological responses of circum-Arctic peatlands to post-industrial climate warming and permafrost degradation. Our results suggest that shrubification of circum-Arctic peatlands has primarily occurred alongside surface drying, resulting from Holocene climate shifts, autogenic peat accumulation, and permafrost aggradation. Future shrubification of circum-Arctic peatlands under 21st century climate change will likely be spatially heterogeneous, and be most prevalent where dry microforms persist.

© 2023 The Authors. Published by Elsevier Ltd. This is an open access article under the CC BY license (http://creativecommons.org/licenses/by/4.0/).

1. Introduction

Twenty-first century climate change is projected to drive widespread vegetation shifts in permafrost peatlands, which presently cover 1.7 ± 0.5 million km^2 and contain 185 ± 70 Gt carbon (C) (Hugelius et al., 2020). Permafrost (perennially frozen ground) renders these vast, fragile carbon stores vulnerable to warming, because thaw-induced surface collapse can drive peatland inundation, which strengthens methane emissions (Heffernan et al., 2022; Holmes et al., 2022). Future peat carbon release may be partially offset by increased plant productivity under warming climates and a poleward shift in woody vegetation, termed shrubification (Myers-Smith et al., 2015; Mekonnen et al., 2021). Shrubification has been widely recognised across upland tundra in response to late-20th century climate change by decadal observations and satellite imagery (Myers-Smith and Hik, 2018; Chen et al., 2021; Mekonnen et al., 2021), although permafrost thaw in lowland tundra has driven thermokarst formation and succession towards graminoid-dominated vegetation (Magnússon et al., 2021; Heijmans et al., 2022). Peatlands represent poorly-

* Corresponding author.
E-mail address: gy15ref@leeds.ac.uk (R.E. Fewster).

https://doi.org/10.1016/j.quascirev.2023.108055
0277-3791/© 2023 The Authors. Published by Elsevier Ltd. This is an open access article under the CC BY license (http://creativecommons.org/licenses/by/4.0/).

drained environments that are often resistant to succession until ecohydrological thresholds are surpassed (Belyea, 2009; Swindles et al., 2015) and may therefore exhibit less linear vegetation transitions under warming climates than mineral-soil tundra. Experimental studies suggest that climate warming and drought increase peatland suitability for shrub and tree encroachment owing to deeper water tables, longer growing seasons, thicker active layers, and restricted moss growth (Heijmans et al., 2013; Limpens et al., 2014b, 2021; Holmgren et al., 2015). Shrubs and trees also survive most effectively on raised peatland surfaces, such as hummocks formed of *Sphagnum* sect. *Acutifolia* (Pouliot et al., 2011; Holmgren et al., 2015). During recent decades, many circum-Arctic peatlands have evidenced surface drying (Zhang et al., 2022), while abundances of *Sphagnum* sect. *Acutifolia* have rapidly increased in Canadian permafrost regions (Magnan et al., 2018, 2022) and the European sub-Arctic (Piilo et al., 2022), providing potentially suitable environments for peatland shrubification. Indeed, some core-based palaeoreconstructions of the recent past have identified shrubs expanding in high-latitude peatlands in North America following late-20th century warming (Gałka et al., 2018; Sim et al., 2019), but no study has yet quantified the broader spatial extent of shrubification in circum-Arctic peatlands, or its long-term context.

Peatland vegetation shifts have important implications for carbon cycling, peat decomposition, and permafrost dynamics (Loisel et al., 2014; Treat et al., 2016). Herbaceous-dominated fens generally exhibit high methane emissions and decay rates (Treat et al., 2021), meaning that *Sphagnum*-dominated bogs are overall more effective carbon sinks (Loisel and Bunsen, 2020; Holmes et al., 2022; Magnan et al., 2022). Tree and shrub establishment on peatlands can substantially increase aboveground biomass and, like *Sphagnum*, woody material is highly resistant to decay (van Breemen, 1995; Camill et al., 2001; Moore et al., 2007). Conversely, peatland shrubification also increases fuel for wildfires, which can combust deep peat carbon in dry sites (Turetsky et al., 2015) and accelerate peat permafrost thaw (Zoltai, 1993; Gibson et al., 2018). Thaw can reverse hydroseral succession (the transition from open waterbodies to fens and bogs), creating saturated depressions that restrict growth of woody vegetation and become recolonised by hydrophilic *Sphagnum* and sedges (Camill, 1999; Minke et al., 2009; Varner et al., 2022), although ice-wedge degradation can also increase lateral drainage (Olefeldt et al., 2021). Therefore, a clear understanding of both recent and long-term successional trends is vital for predicting the future vulnerability of circum-Arctic peatlands.

Plant macrofossils record the past composition of *in situ* plant communities, and enable the study of past changes in peatland vegetation composition (Mauquoy et al., 2010). In a recent compilation by Treat et al. (2016), more than half of the 280 studied peatlands showed fen−bog transitions (FBTs) during the Holocene, while permafrost aggradation in boreal and tundra peatlands resulted in vegetation communities akin to permafrost-free bogs and fens, respectively. A subsequent reanalysis by Treat and Jones (2018) of the same catalogue showed that permafrost aggraded most rapidly in northern peatlands during neoglaciation and the Little Ice Age (LIA), which has been linked to a 20% reduction in methane emissions (Treat et al., 2021). However, these studies did not analyse compositional changes in Holocene peatland vegetation, but rather identified changes in wetland types and primary vegetation, based on the dominant macrofossil component (>30%) or lithological description of peat layers (Treat et al., 2016; Treat and Jones, 2018). Woody vegetation rarely comprised the dominant peat-forming material in any of the studied wetland types (Treat et al., 2016), so past peatland shrubification trends may have been concealed by this approach. Magnan et al. (2022) collated data on plant macrofossil composition from peatlands in Quebec for the last ~200 years and found no evidence of enhanced peatland shrubification under late 20th-century warming, but rather a rapid, northwards expansion of *Sphagnum*. The findings from this study in Quebec contrast recent palaeoecological reconstructions of shrub expansion in other areas, such as northern Alaska (Gałka et al., 2018) and High Arctic Canada (Sim et al., 2019); therefore, the spatiotemporal dynamics of late-Holocene peatland shrubification warrant further investigation.

Existing palaeoecological syntheses have not yet analysed Holocene peatland shrubification at continental scales, and many recently published plant macrofossil records have not been included in previous palaeoecological compilations. Here, we compile and analyse a catalogue of 76 previously-published plant macrofossil records from peatlands across the circum-Arctic permafrost region to explore proportional changes in peatland vegetation during the Holocene. Our analysis provides long-term context for recent observations of shrubification and *Sphagnum* expansion in circum-Arctic peatlands.

2. Methods

2.1. Dataset compilation

We used a structured literature search to collate published plant macrofossil records from peatlands across the circum-Arctic permafrost region. We searched Google Scholar for the terms “permafrost”, “peatland”, “plant macrofossil”, “paleoecology” in conjunction with names of selected regions (e.g., Fennoscandia), countries (e.g., Sweden), states (e.g., Alaska), and provinces and territories (e.g., Nunavut) until June 2022. We selected peat core records from peer-reviewed studies that: i) were located within the circum-Arctic permafrost zone (Brown et al., 2002); ii) contained peat depth and proportional plant macrofossil composition (%) information; and iii) reported uncalibrated radiocarbon (^{14}C) dates. We only considered cores with at least two radiometric dates. We prioritised cores for which raw data are available in the public domain. To reduce bias towards peatlands where multiple plant macrofossil records existed, we selected a single core for each site based on a combination of chronological detail, sampling resolution, core length, proximity to the peatland's centre, and an absence of obvious disturbances in the palaeoecological record (e.g. water-filled voids and stratigraphic unconformities). We grouped cores into broad regional subgroups according to geographical boundaries and core locations (Fig. 1) and determined the zone of contemporary permafrost coverage for each site using the Circum-Arctic Map of Permafrost and Ground-Ice Conditions, Version 2 (Brown et al., 2002). Contemporary permafrost coverage is categorised as continuous (90−100%), discontinuous (50−90%), sporadic (10−50%), or isolated (<10%) (Brown et al., 2002). Plant macrofossils represent *in situ* peatland vegetation (Mauquoy et al., 2010), so our approach does not seek to characterise the full spatial heterogeneity found within complexes of circum-Arctic peatlands. Rather, we explore broad-scale trends in Holocene peatland vegetation change using a subset of well-dated, directly-comparable plant macrofossil records from across the circum-Arctic permafrost region.

From our selection criteria, we assembled published Holocene plant macrofossil data from 76 peat cores (supplementary dataset S1), including 35 cores not included in previous meta-analyses; and 41 cores previously analysed by Treat and Jones (2018) and/or Magnan et al. (2022). Published site descriptions indicate that our selected cores were sampled from a broad range of permafrost and permafrost-free peat types. However, in common with previous peatland syntheses (Loisel et al., 2014; Treat et al., 2016; Magnan et al., 2022), suitable records from fens (n = 11) were less readily

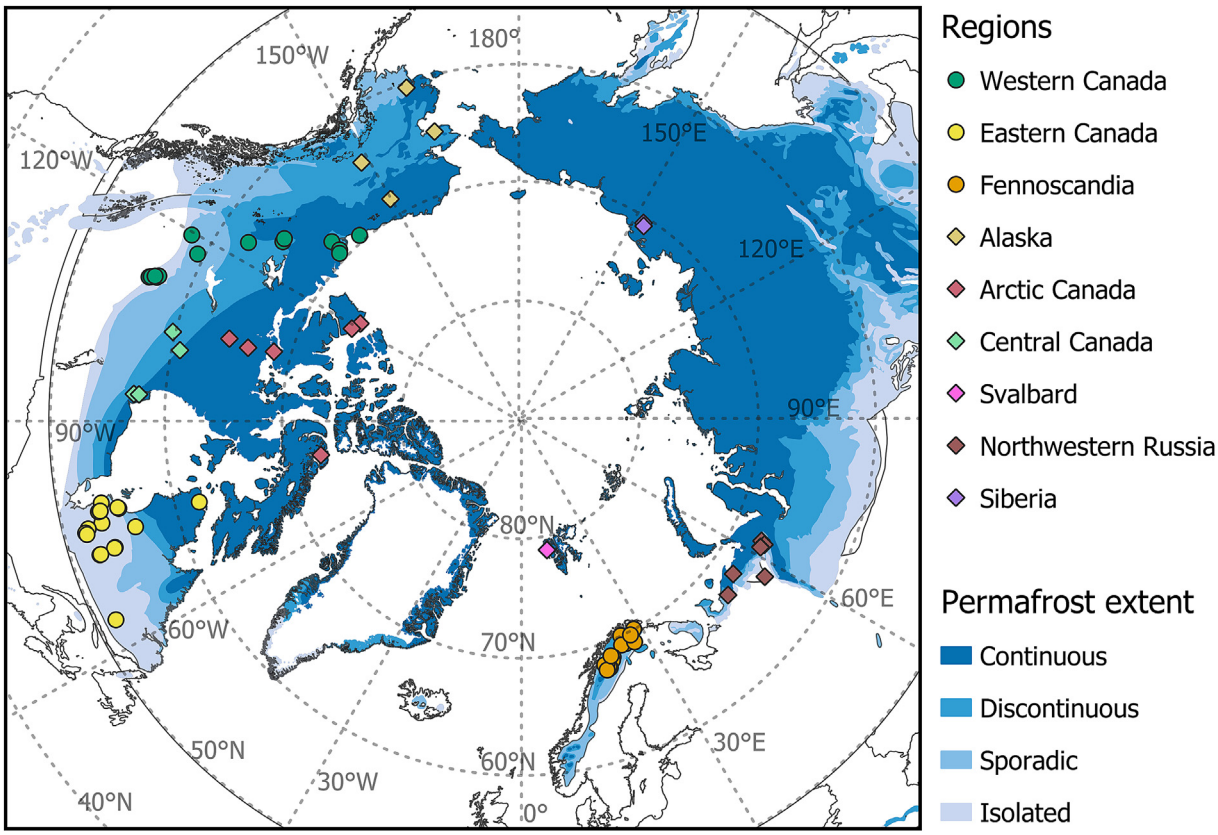

Fig. 1. Distribution of the 76 compiled cores across the circum-Arctic permafrost region, coloured by regional grouping. Circles represent sites used in the regional analyses in Figs. 3 and S2. Extent of contemporary permafrost coverage derived from Brown et al. (2002).

available than for bogs (n = 19) and palsas/peat plateaus (peat-covered frost mounds) (n = 36), likely due to the difficulty of recovering useable samples from saturated fen peats. The collated plant macrofossil records were primarily extracted from *Sphagnum* microhabitats (e.g., hummocks, lawns), partly because shrub and tree roots are more difficult to core through, which may cause some underestimation of recent peatland shrubification in our analyses. Additionally, only nine cores are from polygon mires, which are found in remote northern extremes in cold climates (Fewster et al., 2022). Reconstructions from permafrost peatlands can be hindered by slow net peat accumulation, and even net peat loss during some periods (Väliranta et al., 2021). The temporal lengths of records from permafrost peatlands can also be limited where only unfrozen, active-layer peats are sampled above the local frost table (Zhang et al., 2020; Sim et al., 2021). The peat cores in our dataset are from North America (n = 47) and Eurasia (n = 29), and span contemporary zones of permafrost coverage (continuous, n = 19; discontinuous, n = 21; sporadic, n = 16; isolated, n = 20) (Fig. 1). However, the spatial representation of suitable plant-macrofossil records varied across the circum-Arctic, with a majority of cores located in western Canada (n = 14), eastern Canada (n = 19), and Fennoscandia (n = 19). Conversely, published records of relative plant-macrofossil compositions were rare across Alaska (n = 4), Arctic Canada (n = 6), and Siberia (n = 2), where polygon mires are most abundant (Minke et al., 2007; Peregon et al., 2008).

For each core, we compiled information on peat sampling depth, radiometric chronological controls, plant macrofossil proportions (%) at the taxonomic resolution reported by the original authors, and relevant in-text site descriptions. Plant macrofossil assemblages were recorded by the original authors using standard techniques. We omitted plant macrofossil counts from our analyses (e.g., numbers of fruits and seeds), because these counts cannot be compared directly to relative abundance data, which summarise the major peat forming components through time. Our analyses may therefore underestimate some phases of peatland shrubification where the presence of woody vegetation was only indicated in count data. Additionally, we omitted plant macrofossil data from basal, non-peat sediments. Where numerical plant macrofossil datasets were unavailable in the public domain, we extracted plant macrofossil information from stratigraphic diagrams using WebPlotDigitzer (Rohatgi, 2021).

To enable comparisons of peatland vegetation between cores, we grouped the plant macrofossil data into four plant functional types (PFTs) previously used by Treat et al. (2016): woody (e.g., shrubs, trees, ligneous roots), herbaceous (e.g., grasses, *Equisetum*, and Cyperaceae), non-*Sphagnum* mosses (e.g., brown and feather mosses), and *Sphagnum* spp.. Because not all plant macrofossil records were recorded to species level, we did not differentiate between *Sphagnum* functional types (hummock, lawn, hollow) in our analyses. We included an additional group "other" to quantify the combined proportion of ambiguous material (e.g., uncategorised roots) and unidentified organic matter (UOM) resulting from decomposition. When summed, the collated plant macrofossil proportions did not always total 100%, even when we extracted data directly from published datasets. For these samples, we rescaled the relative abundances of each plant macrofossil group recorded by the original authors to a 0–100% scale, by dividing by the sample total. Our final catalogue contains plant macrofossil

records for 2581 distinct samples from 76 cores, and includes 1076 samples compiled into a synthesis dataset for the first time (see supplementary dataset S2).

2.2. Age-depth modelling

We constructed new age-depth models for each core to ensure our peatland chronologies were standardised against the latest radiocarbon calibration curve, IntCal20 (Reimer et al., 2020). For all cores, we collated uncalibrated ^{14}C dates and their associated laboratory errors. We used reported dates of core extraction as surface ages, but for seven cores without such information we estimated surface ages to be three years prior to study publication dates. For 26 cores, near-surface peat layers were dated by high-precision lead-210 (^{210}Pb) chronologies, and where possible we collated calibrated ^{210}Pb ages and errors. We interpret the most recent changes in the 37 cores from present-day sporadic and discontinuous permafrost zones with some caution, because only 10 of these 37 cores were dated with ^{210}Pb chronologies, while 23 of 37 were missing data for the most recent part of the record (1975–2022 CE). By comparison, 28 of the 39 cores from regions of isolated and continuous permafrost included data for this recent period.

For the majority of cores (n = 58/76), where at least four uncalibrated radiocarbon dates were available, we constructed Bayesian age-depth models using the rbacon package (v.2.5.7) (Blaauw and Christen, 2011) in R v.4.1.3 (R Core Team, 2022). For six cores, where calibrated ^{210}Pb dates were unavailable but sufficient data on ^{210}Pb activity, laboratory errors, and bulk density were accessible, we derived age-depth models using the rplum package (v.0.2.2) (Aquino-López et al., 2018). A Bayesian approach was deemed unsuitable for cores with fewer than four dates, and so for the 12 cores that reported only two or three radiocarbon dates we instead developed classical age-depth models, using the clam package (v.2.4.0) (Blaauw, 2010). Of the 12 age-depth models we constructed in clam, 10 were for cores located in regions of present-day continuous and discontinuous permafrost. We calculated the calibrated age of each sample according to the probability estimates provided by each age-depth model, and do not therefore include chronological uncertainties in our subsequent analyses. Information on the prior settings used for our Bayesian age-depth models, and the regression functions used for our classical models, are presented in Figs. S4–S79.

2.3. Statistical analysis

To investigate long-term trends of peatland vegetation change during the Holocene, we binned the plant macrofossil relative abundance data (%) into non-overlapping 200-year age bins using calibrated dates derived from the age-depth models described in section 2.2., above. To ensure that cores with greater temporal sampling frequency did not distort the binned mean across sites, we calculated the mean of any samples from the same core in the same timestep prior to binning, following Magnan et al. (2022). To identify shorter-term shifts, we also binned the plant macrofossil assemblages into 50-year bins, although the binned data rarely comprised a continuous record for every 50-year timestep. Because our 200-year binned data exhibited greater site replication for each timestep (see Figs. S1–3 for the temporal distribution of core records), we conducted all time-series analyses at a 200-year resolution and present the equivalent 50-year data as supplementary scatter plots.

We also calculated normalised binned plant macrofossil records for each core, which emphasised the direction of change in PFT relative abundance rather than the absolute magnitude. This approach was useful for identifying subtle but potentially important shifts in PFTs with low abundance, because the coexistence of several PFTs at the time of peat formation may obscure trends in non-dominant PFTs in data averaged across multiple sites. For example present-day treed peat plateaus often exhibit an understory of *Sphagnum*, non-*Sphagnum* mosses and lichens (Jones et al., 2017), meaning woody vegetation rarely comprises a dominant peatland-forming component in these sites (Treat et al., 2016), except in rootlet peat layers (Sannel and Kuhry, 2008). Our normalisation approach rescaled the maximum binned relative abundance of each PFT within each core to 100%, and was calculated as:

$$N_{i,j,t} = \frac{A_{i,j,t}}{A_{i,j,max}} \times 100 \quad (1)$$

where $N_{i,j,t}$ is the normalised binned relative abundance of PFT i in core j at timestep t; $A_{i,j,t}$ *is* the non-normalised binned relative abundance of PFT i in core j at timestep t; and $A_{i,j,max}$ is the maximum non-normalised binned relative abundance of PFT i in core j throughout the core record.

We then combined $N_{i,j,t}$ and $A_{i,j,t}$ values between multiple cores to establish trends at different spatial scales. We considered: i) the circum-Arctic (Figs. 2 and S1), ii) geographical regions with at least 10 cores (i.e. western Canada, eastern Canada, and Fennoscandia) (Figs. 3 and S2); and iii) present-day permafrost zones (Brown et al., 2002) (Figs. 4 and S3). Within each grouping of cores, for each PFT i at each 200-year timestep t, we calculated the between-core sum of $A_{i,j,t}$; the between-core mean of $N_{i,j,t}$, which we refer to as the mean normalised relative abundance ($MNRA_{200}$); and the between-core standard error of $N_{i,j,t}$. We also calculated the between-core mean of $N_{i,j,t}$ for each 50-year timestep, which we refer to as $MNRA_{50}$ (presented in Figs. S1–3). We excluded three cores from our normalised 200-year trends that only contained data for the most recent 200-year timestep, but included these cores in our normalised 50-year analysis. To show the effect of our data normalisation, we also present the between-core mean of $A_{i,j,t}$ at 50-year and 200-year intervals for each core grouping in Figs. S1–S3.

We define Holocene subdivisions as early (~11700–~8200 years BP), middle (~8200–~4200 years BP), and late (~4200 years BP–present) (Walker et al., 2019). Henceforth, we report ages as 200-year bin midpoints, unless otherwise specified, and abbreviate "calibrated years BP" to "years BP".

To identify associations between PFTs, we conducted a non-metric multidimensional scaling (NMDS) analysis with the Bray-Curtis dissimilarity index using the vegan library v2.6–2 in R (Oksanen et al., 2022) (Fig. 5). For this analysis, we assessed the between-core mean of $A_{i,j,t}$ for each PFT i at 50-year intervals, averaged across all available cores during the Holocene (since ~11700 years BP) (Fig. S1c), because these data provided a much greater sample size (n = 228) than our equivalent 200-year binned data (n = 59). We limited our ordination to two dimensions to aid interpretability, while ensuring the ordination stress of our final solution was <0.2, following Clarke (1993).

3. Results

3.1. Overall spatiotemporal changes in vegetation

The number of peatland sites represented by our binned 200-year timesteps increased throughout the Holocene from four cores at ~11000 years BP to 61 cores at ~0 years BP (Fig. S1a). Relative changes in peatland vegetation during the early-Holocene should be interpreted with some caution because of the low availability of core records, particularly in regions of present-day continuous and isolated permafrost (Figs. S3a and d). We

therefore focus our interpretations primarily on changes to vegetation composition during the mid- and late-Holocene, when the number of core records increased (Fig. S1a). Additionally, 11 cores in our database contain no data before ~400 years BP. During the full length of peat core records, the 200-year binned relative abundance of herbaceous taxa decreased in 59 cores, while woody vegetation and *Sphagnum* increased in 44 and 41 cores, respectively. Proportions of woody vegetation and *Sphagnum* predominantly increased in cores extracted from palsas/peat plateaus (woody, $n = 24/36$; *Sphagnum*, $n = 21/36$) and bogs (woody, $n = 13/19$; *Sphagnum*, $n = 13/19$).

Overall, circum-Arctic peatlands evidenced a shift from communities dominated by herbaceous taxa prior to ~4000 years BP, to those composed primarily of *Sphagnum,* non-*Sphagnum* mosses and woody vegetation at ~0 years BP (Figs. 2 and S1). Transitions from herbaceous communities to assemblages dominated by *Sphagnum* and non-*Sphagnum* mosses accelerated from ~600 years BP, although woody expansion continued more gradually (Fig. 2b), reflecting heterogeneity between geographical regions and present-day permafrost zones (see section 3.2 below). The $MNRA_{200}$ of PFTs averaged across all sites indicates a consistent expansion of woody vegetation from ~8200 years BP to present (Fig. 2b). However, recent increases to woody material were often of a smaller magnitude than *Sphagnum* and non-*Sphagnum* mosses, possibly due to the bias in field sampling towards *Sphagnum*-dominated microhabitats, which resulted in a slight decline in non-normalised mean woody abundance at ~0 years BP (Figs. 2a and S1b). The $MNRA_{200}$ of woody vegetation increased steadily during ~8200–3800 years BP and since ~1800 years BP, although a temporary decline occurred during ~3600–2600 years BP. Our results indicate a substantial increase in the $MNRA_{200}$ of *Sphagnum* between ~7400 and 3600 years BP, when *Sphagnum* became the dominant PFT for the first time (Fig. S1), following a steady reduction in herbaceous taxa across the same period (Fig. 2b). *Sphagnum* expansion in circum-Arctic peatlands occurred in three main phases during the mid- to late-Holocene: during ~7400–4800 years BP, ~3400–2600 years BP, and since ~800 years BP. *Sphagnum* expansion temporarily slowed during ~1600–800 years BP, enabling herbaceous taxa to briefly re-emerge as the dominant PFT (Fig. S1). However, following a recent rapid decline, herbaceous taxa became the least abundant PFT at ~0 years BP, while the $MNRA_{200}$ of *Sphagnum* increased sharply after ~600 years BP. Non-*Sphagnum* mosses evidenced comparatively low $MNRA_{200}$ during ~5800–400 years BP, but increased rapidly thereafter, with the greatest expansion occurring in cores from the continuous permafrost zone (see section 3.3 below).

Our NMDS ordination highlighted the underlying dissimilarity between PFTs in circum-Arctic peatlands and presented a temporal gradient of vegetation succession along Axis 1 (Fig. 5). Binned mean assemblages from before ~6000 years BP were commonly distributed to the right of the ordination space, alongside the herbaceous and non-*Sphagnum* moss PFTs. All binned mean assemblages since ~2000 years BP recorded negative Axis 1 scores and were closely clustered, with low Axis 1 scores evidencing close association with *Sphagnum* and woody vegetation. Axis 2 indicated further dissimilarity between the PFTs, with *Sphagnum* and non-*Sphagnum* mosses shown to be strongly dissimilar across both axes.

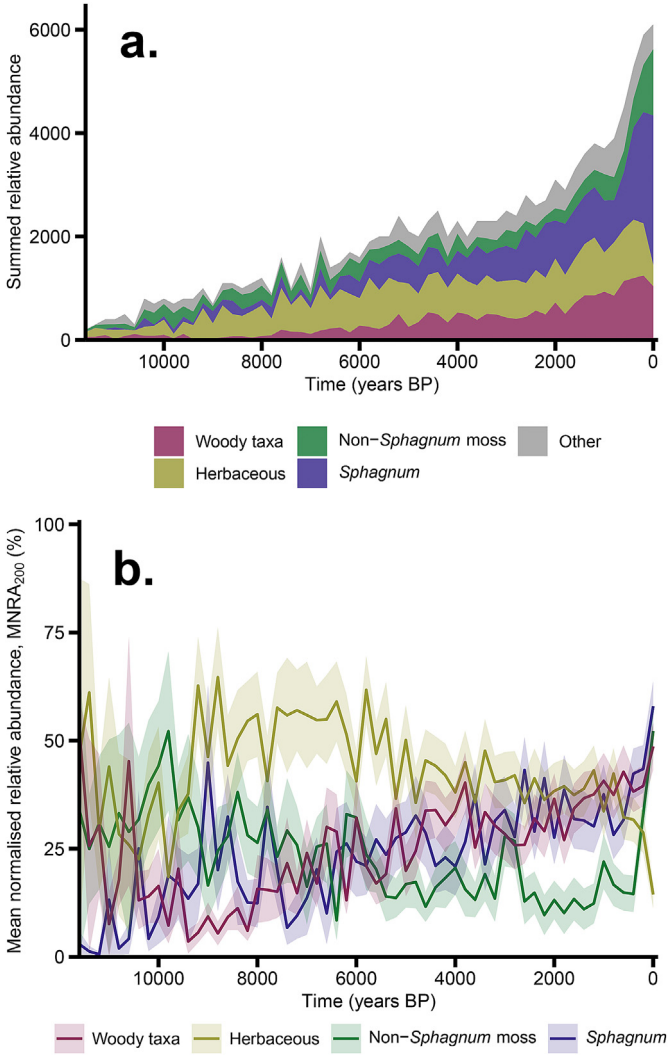

Fig. 2. Holocene vegetation shifts in the studied circum-Arctic peatlands presented in 200-year bins as: (a) the between-core summed relative abundance of plant functional types (PFTs); and (b) the between-core mean normalised relative abundance (%) of PFTs, $MNRA_{200}$, with shading representing the standard error of $MNRA_{200}$. Other refers to unidentified organic matter or ambiguous material. Increasing summed data over time reflects continued peatland initiation (see Fig. S1a for core distribution through time). For details of data normalisation, see methods section 2.3., and for the between-core mean normalised relative abundance in 50-year bins, $MNRA_{50}$, see Fig. S1d.

3.2. Spatiotemporal variation in Holocene shrubification

The $MNRA_{200}$ of woody vegetation gradually increased through the mid- to late-Holocene across the present-day discontinuous, sporadic, and isolated permafrost zones (Figs. 4 and S3), with late-Holocene increases prominent in cores from Fennoscandia and western Canada (Fig. 3). In the discontinuous permafrost zone, woody vegetation in some cores peaked prior to ~10000 years BP (Fig. 4d), for example in early deglaciated regions of Alaska (Hunt et al., 2013) and northwestern Russia (Oksanen et al., 2001). However, during ~9400–8000 years BP the $MNRA_{200}$ of woody vegetation in this zone was generally low. After ~6000 years BP, the $MNRA_{200}$ of woody vegetation in the discontinuous permafrost zone greatly increased, although large fluctuations occurred during this period, with lower abundances particularly evident during ~3600–2200 years BP. Similarly, cores from the sporadic permafrost zone evidenced a consistent expansion of woody vegetation after ~5000 years BP, in parallel with *Sphagnum* increases (Fig. 4f). In the isolated permafrost zone, the $MNRA_{200}$ of woody vegetation primarily increased before ~4000 years BP and remained high throughout the late-Holocene, despite a steady decline after ~600 years BP (Fig. 4h).

The late-Holocene expansion of woody vegetation in the contemporary discontinuous and sporadic permafrost zones was

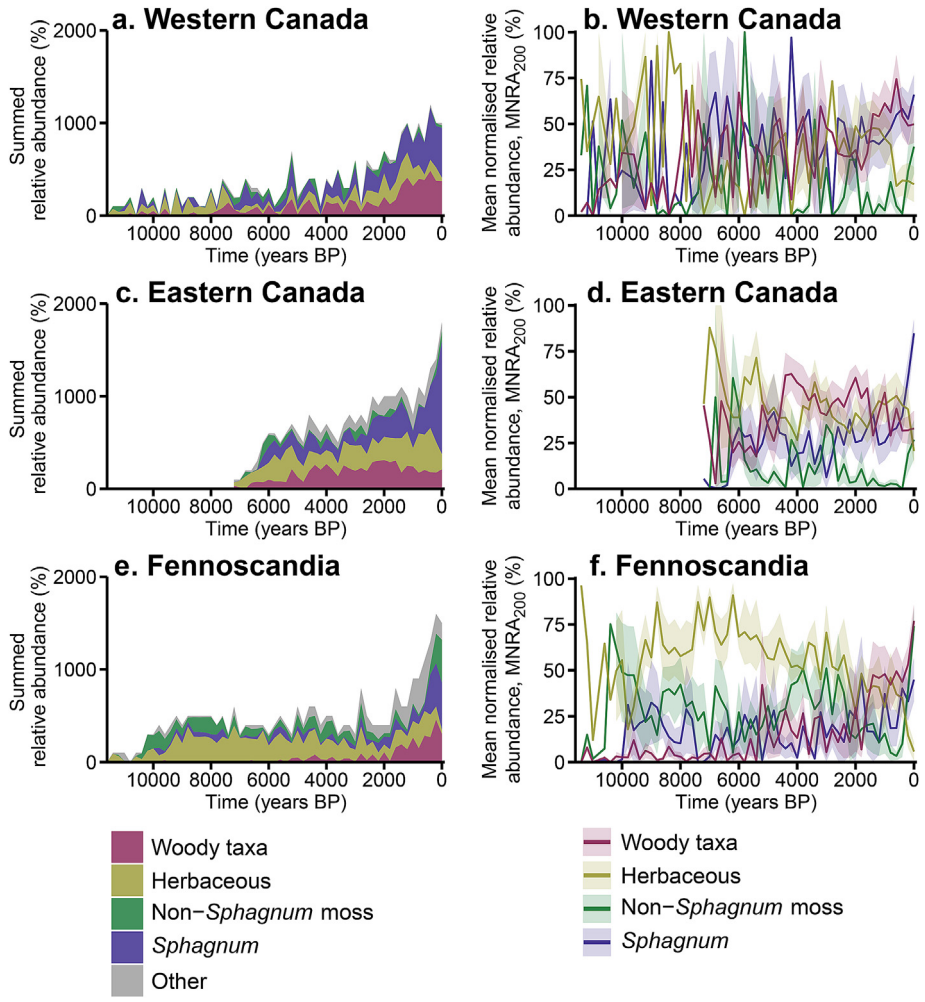

Fig. 3. Spatiotemporal variation in Holocene peatland vegetation shifts between geographic regions (see Fig. 1 for details). The between-core summed relative abundance of plant functional types (PFTs) in 200-year bins for cores from (a) western Canada, (c) eastern Canada, and (e) Fennoscandia. Other refers to unidentified organic matter or ambiguous material. Increasing summed data over time reflects continued peatland initiation (see Figs. S2a–c for core distribution through time). The between-core mean normalised relative abundance (%) of PFTs in 200-year bins, $MNRA_{200}$, for cores from (b) western Canada, (d) eastern Canada, and (f) Fennoscandia. Shading represents the standard error of $MNRA_{200}$. For details of data normalisation, see methods section 2.3., and for the between-core mean normalised relative abundance in 50-year bins, $MNRA_{50}$, see Figs. S2j-l.

largely driven by increases in Fennoscandia, where 49% ($n = 18/37$) of cores from these permafrost zones are located. The $MNRA_{200}$ of woody vegetation was low in Fennoscandia throughout the early- and mid-Holocene, but increased rapidly during ~1800–1400 years BP and after ~400 years BP (Fig. 3f). A comparable increase in the $MNRA_{200}$ of woody vegetation occurred in western Canada during ~1800–600 years BP, although proportions in this region have subsequently declined (Fig. 3b). Our results for the isolated permafrost zone were dominated by cores located in eastern Canada ($n = 14/20$), where a longer-term decline in the $MNRA_{200}$ of woody vegetation was indicated from ~2000 years BP to present (Fig. 3d).

In contrast, five cores from the present-day continuous permafrost zone exhibited maximum values for the 200-year binned relative abundance of woody vegetation between ~6600 and 3000 years BP (Fig. 4b), while four cores from this zone exhibited no woody material throughout the entire core record (Ellis and Rochefort, 2004; Nakatsubo et al., 2015; Sim et al., 2019). The density of core records for the continuous permafrost zone in each 200-year timestep prior to ~2000 years BP was low, but increased thereafter (Fig. S3a). Between ~2000 and ~200 years BP the $MNRA_{200}$ of woody vegetation persisted at relatively low levels in the continuous permafrost zone, but noticeably increased at ~0 years BP when six cores recorded maximum 200-year binned relative abundances of woody vegetation.

Of the 52 cores that contained data for both the ~200 and ~0 years BP timesteps, a comparable number evidenced recent woody expansion ($n = 23$) and decline ($n = 24$), with both trajectories evident across all permafrost zones. Very recent shifts in vegetation composition should be interpreted with some caution, because relatively undecomposed organic matter may be present in some near-surface samples. Despite this, a greater number of cores in eastern Canada between ~200 and ~0 years BP evidenced reductions in woody vegetation ($n = 8$) than increases ($n = 5$), coinciding with rapid *Sphagnum* expansion (see section 3.3 below). Considering all records, we found that maximum values for the 200-year binned relative abundance of woody vegetation were reached at ~0 years BP in 16 cores, of which a majority were located northwards of 65°N ($n = 11/16$), for example in Fennoscandia (Sim et al., 2021), Arctic Canada (Sim et al., 2019), Alaska (Gałka et al., 2018), and Siberia (de Klerk et al., 2011).

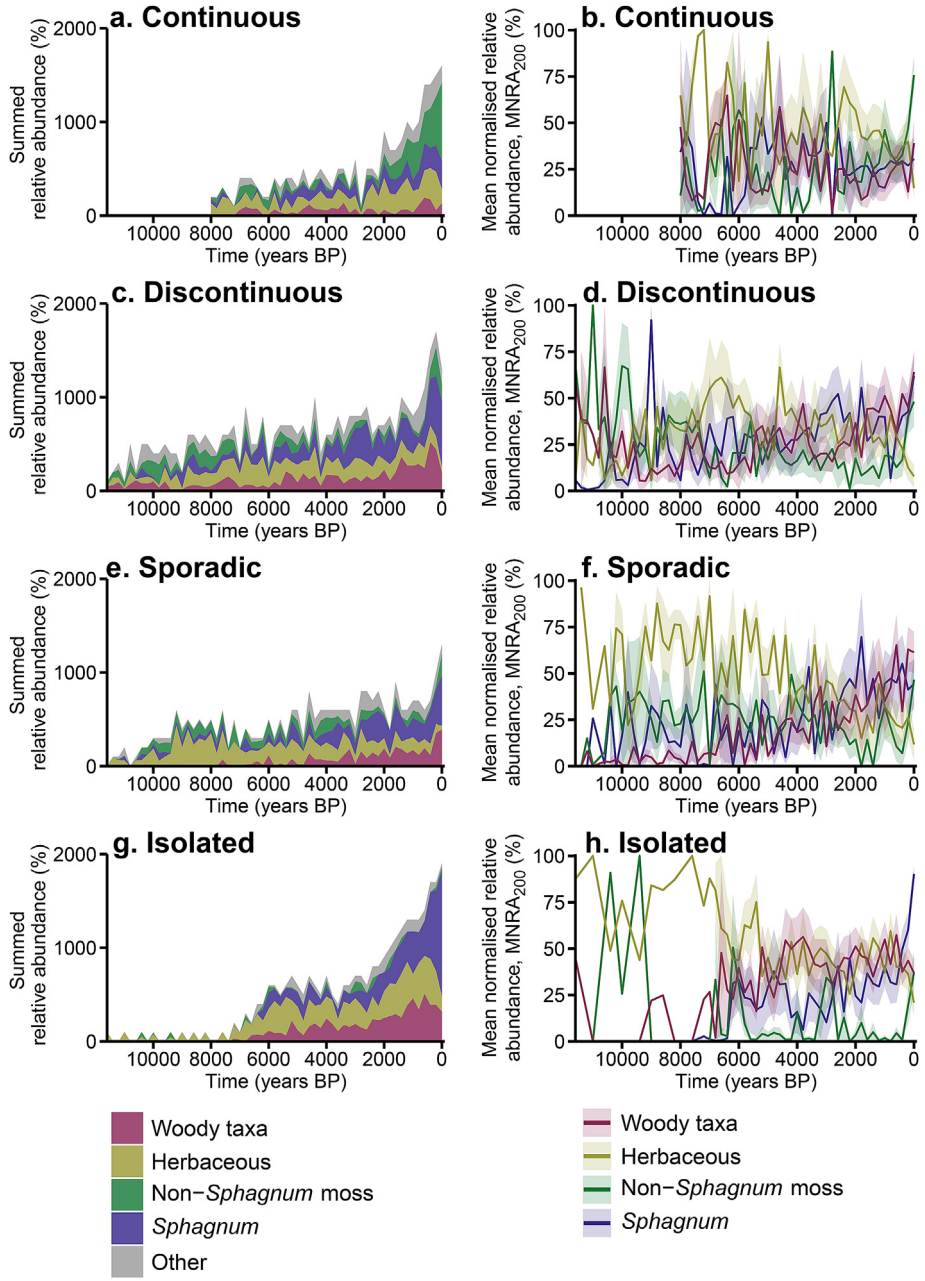

Fig. 4. Spatiotemporal variation in Holocene peatland vegetation shifts between present-day permafrost zones. The between-core summed relative abundance of plant functional types (PFTs) in 200-year bins for cores from the (a) continuous, (c) discontinuous, (e) sporadic, and (g) isolated permafrost zones. Other refers to unidentified organic matter or ambiguous material. Increasing summed data over time reflects continued peatland initiation (see Figs. S3a–d for core distribution through time). The between-core mean normalised relative abundance (%) of PFTs in 200-year bins, $MNRA_{200}$, for cores from the (b) continuous, (d) discontinuous, (f) sporadic, and (h) isolated permafrost zones. Shading represents the standard error of $MNRA_{200}$. For details of data normalisation, see methods section 2.3., and for the between-core mean normalised relative abundance in 50-year bins, $MNRA_{50}$, see Figs. S3m-p.

3.3. Holocene moss expansion in permafrost peatlands

Peatlands in regions of contemporary discontinuous, sporadic and isolated permafrost exhibited late-Holocene shifts from herbaceous- to *Sphagnum*-dominated assemblages, while peatlands in the continuous permafrost zone indicated rising abundances of non-*Sphagnum* mosses from ~1800 years BP (such as *Calliergon* spp., *Dicranum* spp. and *Scorpidium* spp.) (Fig. 4). During the early- and mid-Holocene, the $MNRA_{200}$ of herbaceous taxa was high across the circum-Arctic, but declined steadily in regions of continuous, discontinuous and sporadic permafrost from ~2400 years BP, ~4600 years BP, and ~5800 years BP, respectively. Conversely, the $MNRA_{200}$ of herbaceous taxa remained stable in the isolated permafrost zone until ~400 years BP, but decreased sharply thereafter. Our dataset indicates a steady expansion in the $MNRA_{200}$ of *Sphagnum* in regions of discontinuous and sporadic permafrost during ~4600–2600 years BP and ~2800–1800 years BP, respectively. The $MNRA_{200}$ of *Sphagnum* in the discontinuous and sporadic permafrost zones subsequently declined until ~800 years BP and ~1200 years BP, respectively, when herbaceous communities temporarily recovered (Figs. 4c–f). In the isolated permafrost zone, the $MNRA_{200}$ of *Sphagnum* has increased consistently since ~3000

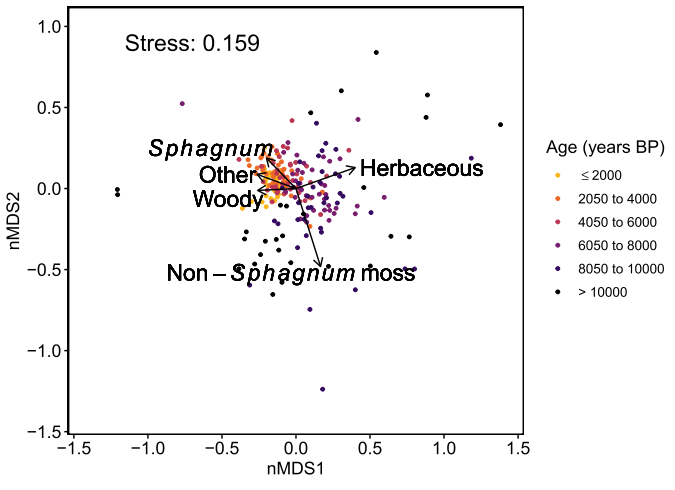

Fig. 5. Non-metric multidimensional scaling (NMDS) plot showing Bray-Curtis dissimilarities between the mean relative abundance (%) of plant functional types in 50-year bins, averaged across all available cores. Other refers to unidentified organic matter or ambiguous material. For the time-series of these data, see Fig. S1c. Binned samples are colour-coded by age (years BP).

years BP and rapidly since ~600 years BP. Continued late-Holocene expansion of *Sphagnum* meant that at ~0 years BP, *Sphagnum* was the dominant PFT in the studied cores from regions of discontinuous, sporadic, and isolated permafrost (Figs. 4c,e,g).

Conversely, in the continuous permafrost zone non-*Sphagnum* mosses were the dominant PFT at ~0 years BP (Fig. 4a), following consistent increases from ~1800 years BP, which accelerated after ~400 years BP (Fig. 4b). By comparison, the $MNRA_{200}$ of *Sphagnum* in the continuous permafrost zone has persisted at low levels since ~2400 years BP. Rapid increases to the $MNRA_{200}$ of non-*Sphagnum* mosses also occurred after ~400 years BP in cores from the discontinuous, sporadic, and isolated permafrost zones, although absolute increases in relative abundance in these cores were lesser than those from the continuous permafrost zone (Figs. 4 and S3).

Our regional analyses indicate moderate *Sphagnum* abundance in cores from eastern Canada from ~6000 years BP, while *Sphagnum* expansion in Fennoscandian cores primarily occurred during ~2400–1800 years BP and after ~1200 years BP (Fig. 3). After ~1000 years BP, the $MNRA_{200}$ of *Sphagnum* increased steadily in western Canada and rapidly in eastern Canada, with eight cores from these regions exhibiting maximum values for the 200-year binned relative abundance of *Sphagnum* at ~0 years BP. In Fennoscandia, a steady decline in the $MNRA_{200}$ of herbaceous taxa from ~6200 years BP accelerated from ~400 years BP, when the $MNRA_{200}$ of non-*Sphagnum* mosses substantially increased (Fig. 3f).

4. Discussion

4.1. Drivers of Holocene peatland vegetation dynamics

4.1.1. Early succession (prior to ~6000 years BP)

Cores in our plant macrofossil compilation with basal dates indicate distinct spatial patterns of peat initiation prior to ~6000 years BP, when peatlands primarily established in early-deglaciated regions of Fennoscandia (Kjellman et al., 2018; Sannel et al., 2018), northwestern Russia (Oksanen et al., 2001, 2003; Väliranta et al., 2003), western Canada (Vardy et al., 1997, 1998; Kettles et al., 2003; Bauer and Vitt, 2011) and Alaska (Hunt et al., 2013). Although only seasonally-thawed peats from the active layer were sampled from some permafrost peatland sites, these spatiotemporal patterns of peatland development corroborate previous findings (MacDonald et al., 2006; Morris et al., 2018; Treat et al., 2021). Early peat initiation in these regions occurred during warming growing seasons (Morris et al., 2018) following the onset of the Holocene Thermal Maximum (HTM) at ~11000–8000 years BP (Kaufman et al., 2004; Weckström et al., 2010; Salonen et al., 2011), with proxy records indicating that generally warm, stable climates continued in these regions until ~5000 years BP (Korhola et al., 2002; Salonen et al., 2011; Kaufman et al., 2016; Sejrup et al., 2016). In Fennoscandian cores, high abundances of herbaceous taxa and non-*Sphagnum* mosses from inception (Figs. 3e and f) have been inferred to represent direct peat establishment onto wet mineral substrates (Kjellman et al., 2018; Sannel et al., 2018). Conversely, cores compiled from northwestern Russia and western Canada indicated peat initiation by terrestrialisation (infilling of waterbodies), with aquatic plants pre-dating fen species (Vardy et al., 1997, 1998; Oksanen et al., 2001, 2003), or paludification of existing forests, indicated by woody basal materials (Oksanen et al., 2001; Väliranta et al., 2003). Extensive peat initiation is thought to have started later in eastern Canada between ~8000 and ~4000 years BP (Payette, 1984; MacDonald et al., 2006; Fewster et al., 2020), following the final deglaciation of the Laurentide Ice Sheet during ~8200–6700 years BP (Ullman et al., 2016). Core records for eastern Canada in our synthesis begin from ~7200 years BP (Figs. 3c and d) and indicate peat initiation through paludification (Robitaille et al., 2021) and terrestrialisation (Beaulieu-Audy et al., 2009; Langlais et al., 2021).

Our dataset contains limited evidence for woody expansion in circum-Arctic peatlands prior to ~6000 years BP, despite existing evidence that treelines were located farther north than present in early-deglaciated regions during the HTM (Payette and Lavoie, 1994; MacDonald et al., 2000). High peaks in the $MNRA_{200}$ of woody vegetation prior to ~10000 years BP in the contemporary discontinuous permafrost zone more likely indicate early paludification or alder fen formation than peatland shrubification, because abundances quickly declined and remained low during 9400–8000 years BP (Figs. 4c and d). A previous review of subfossil peatland tree chronologies suggested that a scarcity of tree subfossils for the early-Holocene resulted from an absence of ombrotrophic peatlands (Edvardsson et al., 2016), likely owing to the generally long timescales required for FBTs (centuries to several millennia) (Beaulieu-Audy et al., 2009; Väliranta et al., 2017; Sannel et al., 2018), although some later-forming cores indicate *Sphagnum fuscum* presence since initiation (Sannel and Kuhry, 2008). Alternatively, woody vegetation may have grown in alder fens, but these wetlands are uncommon in permafrost regions. Indeed, the $MNRA_{200}$ of herbaceous taxa was high across the circum-Arctic prior to ~6000 years BP (Fig. 2), particularly in cores from Fennoscandia (Figs. 3e and f), where several of the studied peatlands persisted as sedge-dominated fens throughout this period (Kjellman et al., 2018; Sannel et al., 2018). Even alongside the favourable warm climates of the HTM, shrub growth in minerotrophic fens would have been complicated by continuously high water tables, which reduce oxygen availability for roots (Leuschner et al., 2002). However, proportions of woody vegetation did increase in several herbaceous-dominated sites before ~6000 years BP (Oksanen et al., 2001; Väliranta et al., 2003; Vardy et al., 1998, 2005; van Bellen et al., 2011), for example where isolated hummocks provided suitably dry substrates for ligneous root growth (Kjellman et al., 2018).

4.1.2. Mid-to late-Holocene (~6000–~1000 years BP)

After ~6000 years BP, circum-Arctic peatland communities experienced a widespread shift towards *Sphagnum* and woody vegetation (Fig. 2), particularly in regions of present-day discontinuous, sporadic and isolated permafrost (Figs. 4c–f). Across the

Arctic, this period is characterised by neoglacial climate cooling (Seppä and Birks, 2001; Gajewski, 2015; McKay et al., 2018). Multiproxy analyses indicate that the onset of neoglacial cooling was spatially variable, beginning earliest in Fennoscandia and Russia from ~7000 years BP where cooling accelerated after ~2000 years BP (McKay et al., 2018), when binned assemblages in our analyses were primarily associated with *Sphagnum* and woody vegetation (Fig. 5). Treelines retracted to their contemporary geographical limit at ~3500 years BP across much of the Arctic (Payette and Lavoie, 1994; MacDonald et al., 2000), but continued to retreat southwards in Fennoscandia and European Russia after ~3000 years BP (Seppä and Birks, 2001; Fang et al., 2013).

The sharp decline in herbaceous vegetation after ~6000 years BP, and rising abundances of *Sphagnum* across all permafrost zones, is indicative of widespread FBTs and permafrost aggradation across the circum-Arctic from ~7500 years BP (Treat et al., 2021). Autogenic peat accumulation occurred rapidly during the HTM (Jones and Yu, 2010; Yu et al., 2010; Loisel et al., 2014), causing peat surfaces in many sites to rise above local water tables, which facilitated growth of hummock-forming *Sphagnum* and shifts to ombrotrophic conditions during the mid-Holocene (Kuhry, 2008; Beaulieu-Audy et al., 2009; Langlais et al., 2021; Robitaille et al., 2021). These raised, ombrotrophic surfaces likely provided more suitable environments for shrub and tree colonisation than preceding wet fens. The persistence of high herbaceous abundances during ~4000–1200 years BP in regions of present-day continuous permafrost (Figs. 4a and b) may partly be attributed to the initiation of several new peatlands, exhibiting initially wet conditions that favoured growth of sedges and brown mosses (Fritz et al., 2016; Teltewskoi et al., 2016; Gałka et al., 2018). Furthermore, herbaceous-dominated communities persisted in several Fennoscandian cores until ~2400 years BP (Figs. 3e and f), with ombrotrophication of these sites likely delayed by cold and moist neoglacial climates (Seppä and Birks, 2001) and the late aggradation of permafrost in this region (Kjellman et al., 2018; Sannel et al., 2018; Treat and Jones, 2018). Temporary reversions to fen vegetation also occurred in some established *Sphagnum*-dominated peatlands after ~6000 years BP, in response to water table fluctuations (Robitaille et al., 2021) or permafrost degradation (Sannel and Kuhry, 2008), highlighting that peatland succession is not a unidirectional process.

The continued expansion of woody vegetation may also have been facilitated by early peat permafrost aggradation. Previous syntheses indicate steady rates of permafrost aggradation in peatlands across the circum-Arctic from ~9000 years BP, and peat permafrost became widespread in high latitude regions of Alaska, western Canada and Siberia by ~2500 years BP (Treat and Jones, 2018; Treat et al., 2021). In a similar manner to ombrotrophication, permafrost aggradation can create raised surfaces that are conducive to shrub colonisation, for example atop palsas/peat plateaus that exhibit deeper water tables than neighbouring fens (Zoltai and Tarnocai, 1975). Considering all cores in our dataset, original author interpretations suggest that peat permafrost aggradation occurred earliest in cores from western and central Canada (before ~4000 years BP) (Vardy et al., 1998; Sannel and Kuhry, 2008; Bauer and Vitt, 2011), as indicated by alternating *Sphagnum fuscum* and rootlet layers, and rising abundances of Ericaceae. Although evidence exists for peat permafrost occurrence in some parts of northeastern Quebec from ~5500 years BP (Treat and Jones, 2018), pollen records suggest that warm, moist climates persisted in Quebec until ~2000 years BP (Kaufman et al., 2004; Viau and Gajewski, 2009), and most cores compiled for eastern Canada appear to have been permafrost-free throughout the Holocene. Increases to the $MNRA_{200}$ of *Sphagnum* and woody vegetation in eastern Canada after ~6000 years BP were therefore more likely driven by FBTs, accelerated by rapid peat accumulation under favourable climates (Beaulieu-Audy et al., 2009; Robitaille et al., 2021). Furthermore, previous research indicates that peat permafrost aggradation in Fennoscandia and northwestern Russia primarily occurred after ~1000 years BP (Kjellman et al., 2018; Sannel et al., 2018; Treat and Jones, 2018).

The declining $MNRA_{200}$ of woody vegetation in western Canada during ~3200–1800 years BP (Figs. 3a and b) may indicate that cooling climates across the MacKenzie River Basin after ~5000 years BP (Viau and Gajewski, 2009) eventually restricted peatland shrubification through reduced growing season temperatures or rising water tables. Simultaneous increases in *Sphagnum* perhaps reflects their broader tolerance to wet, anoxic conditions, low temperatures, and low nutrient availability (van Breemen, 1995; Gajewski et al., 2001). Alternatively, this temporary woody decline may be explained by peatland wildfires, which increased in frequency and severity in parts of western and central Canada after ~4000 years BP (Zoltai, 1993; Camill et al., 2009; Pelletier et al., 2017), and some cores from these regions evidenced a recurrence of charcoal and burnt materials after ~3600 years BP (Kettles et al., 2003; Sannel and Kuhry, 2008).

4.1.3. Last millennium (since ~1000 years BP)

Peatland vegetation succession accelerated in circum-Arctic peatlands after ~1000 years BP, when late-Holocene climate shifts increased rates of ombrotrophication (Magnan et al., 2022) and peat permafrost aggradation and thaw (Treat and Jones, 2018). In common with previous suggestions by Treat et al. (2016), we identified differing successional pathways between peatlands in boreal and tundra ecoregions, with peatlands in the continuous permafrost zone evidencing a rapid expansion of non-*Sphagnum* mosses from ~1800 years BP (Fig. 4b). Although this late-Holocene expansion of non-*Sphagnum* mosses primarily occurred in polygon mires (Ouzilleau Samson et al., 2010, de Klerk et al., 2011; Teltewskoi et al., 2016; Sim et al., 2019), several cores from palsas/peat plateaus and bogs in Fennoscandia also indicated increased proportions of non-*Sphagnum* mosses in recent centuries (Kjellman et al., 2018; Sannel et al., 2018; Sim et al., 2021) (Figs. 3e and f). In contrast to other permafrost regions, the $MNRA_{200}$ of *Sphagnum* in the continuous permafrost zone remained comparatively low during the last millennium, perhaps indicating that growing seasons at high northern latitudes have been too cold for enhanced *Sphagnum* productivity (Gajewski et al., 2001; Loisel et al., 2012). Alternatively, in some High Arctic wetlands *Sphagnum* growth may have been restricted by high calcium concentrations (Vicherová et al., 2015), which can develop in shallow Arctic peats that overlie carbonate landscapes and that are seasonally inundated by snowmelt and ground-ice melt (Woo and Young, 2006). Recent peatland succession in the studied polygon mires appears to have been strongly influenced by shifts in local hydrology, resulting from permafrost-driven changes to microtopography (Ellis and Rochefort, 2004, de Klerk et al., 2011; Teltewskoi et al., 2016). Recent non-*Sphagnum* moss growth was primarily attributable to hydric moss expansion (e.g., *Calliergon* spp. or *Drepanocladus* spp.) in cores extracted from wet polygon depressions or thawed trenches (Ouzilleau Samson et al., 2010, de Klerk et al., 2011; Sim et al., 2019), and mesic moss expansion (e.g., *Aulacomnium turgidum* and *Dicranum* spp.) in cores from drier, high-centred polygons and ridges (Ellis and Rochefort, 2004; Vardy et al., 2005; Teltewskoi et al., 2016).

Although six cores from the continuous permafrost zone recorded maximum values for the 200-year binned relative abundance of woody vegetation at ~0 years BP, non-normalised woody proportions remained low ($\leq$11%) at this time in many of the available cores from this zone (n = 13/16) (Fig. S3a). This may

suggest that permafrost peatlands in the High and Low Arctic have not, as yet, undergone the widespread shrubification observed in tundra environments (Mekonnen et al., 2021; Heijmans et al., 2022). Notable examples of recent peatland shrubification in regions of continuous permafrost were identified in cores from northern Alaska (Gałka et al., 2018) and a coastal fen in High Arctic Canada (Sim et al., 2021), where binned woody abundances have greatly increased since ~200 years BP. In the latter fen site, woody vegetation was subsequently replaced by non-*Sphagnum* mosses after 2000 CE, a transition previously attributed to the preferential herbivory patterns of Arctic geese (Sim et al., 2019). Phases of increased shrubification also occurred in some polygon mire sites during recent millennia, but predominantly in cores extracted from elevated high-centred polygons and ridges (Vardy et al., 1997, 2005; Teltewskoi et al., 2016), supporting previous observational studies of polygon mire succession (Minke et al., 2009; Wolter et al., 2016). Conversely, core assemblages from low-centred polygons and troughs were dominated by herbaceous taxa and non-*Sphagnum* mosses throughout the Holocene (de Klerk et al., 2011; Sim et al., 2019). These localised depressions commonly exhibit persistent wet conditions, because neighbouring polygon rims create strong hydraulic gradients and act as hydrological barriers within the landscape (Helbig et al., 2013). Furthermore, vegetation compositions in low-centred polygons are more greatly influenced by the hydraulic properties of the underlying mineral soil, particularly where active-layers have deepened, because these sites exhibit shallower peat layers than high-centred polygons and palsas/peat plateaus (Zoltai and Tarnocai, 1975).

Considering all cores in our dataset, the $MNRA_{200}$ of woody vegetation was consistently highest after ~1000 years BP (Fig. 2b), following the warm summer temperatures of the Medieval Climate Anomaly (MCA) in the Arctic during ~1030–890 years BP (Werner et al., 2018). Temperatures varied across the northern hemisphere during the MCA, becoming mild in eastern Canada and northern Europe, but remaining cool across much of Siberia (Mann et al., 2009; Werner et al., 2018). Climatic conditions in Fennoscandia during the MCA were favourable for shrubification, as evidenced by altitudinal upshifts in the *Pinus sylvestris* treeline in Fennoscandia (Hiller et al., 2001; Kullman, 2015). The $MNRA_{200}$ of woody vegetation in the discontinuous and sporadic permafrost zone generally stabilised after ~1000 years BP (Figs. 4c–f) but evidenced continued increases in Fennoscandia after ~400 years BP (Figs. 3e and f). Woody growth in these regions therefore continued during the coldest temperatures of the LIA (~550–100 years BP) (Mann et al., 2009; Werner et al., 2018), when peatland permafrost reached its most southerly extent (Halsey et al., 1995; Treat and Jones, 2018). LIA cooling deepened water tables in some peatlands in western Canada and Fennoscandia, often through climate-induced permafrost aggradation, which resulted in drier peat surfaces favourable for *Sphagnum* and woody encroachment (Magnan et al., 2018; Zhang et al., 2018). By contrast, the declining $MNRA_{200}$ of woody vegetation in eastern Canada after ~2000 years BP coincided with regional increases to precipitation (Viau and Gajewski, 2009; Rodysill et al., 2018) and recent peatland surface wetting (Zhang et al., 2022). For example, reduced evapotranspiration during the LIA caused water tables to rise in some poor fen sites in Quebec, resulting in an expansion of hydrophilic *Sphagnum* (Van Bellen et al., 2013). Furthermore, recent woody decline has occurred in 24 cores across the circum-Arctic since ~200 years BP, during the peak period of Holocene peat permafrost thaw (Magnan et al., 2018; Treat and Jones, 2018).

In agreement with previous studies by Magnan et al. (2018, 2022) and Piilo et al. (2022) our results demonstrated a rapid, concurrent expansion of *Sphagnum* during recent centuries in peatlands from western and eastern Canada and Fennoscandia (Fig. 3), coinciding with the end of the LIA and the onset of recent anthropogenic climate change. Magnan et al. (2018, 2022) demonstrated that peatlands from regions of sporadic and isolated permafrost in eastern Quebec and Alberta widely transitioned from fens to bogs during the 20th century and experienced a rapid expansion of *Sphagnum* sect. *Acutifolia* after 1980 CE in response to recent climate warming and increased evapotranspiration. Our data compilation includes 17 cores from eastern and western Canada that were included in these two studies, a majority of which are located in the isolated permafrost zone ($n = 15$), which explains why our results for this permafrost zone show similarly rapid increases to *Sphagnum* abundance after ~200 years BP (Figs. 4g and h). In some alternative cores from the James Bay Lowlands, Quebec, that were not previously analysed by Magnan et al. (2022), there is evidence of earlier shifts towards *Sphagnum* sect. *Acutifolia* (Beaulieu-Audy et al., 2009, van Bellen et al., 2011), while *Sphagnum fuscum* developed from ~760 years BP in a palsa near Duncan Lake, Quebec (Tremblay et al., 2014). We interpret very recent changes in the isolated permafrost zone with greater confidence than other regions, because 65% of our age-depth models from this permafrost zone ($n = 13/20$) included ^{210}Pb dating profiles for near-surface peats in addition to ^{14}C chronologies, compared to 23% of cores from all other permafrost zones ($n = 13/56$). Slow peat accumulation rates, low sampling resolutions, and intermixing of deceased plant material can also sometimes disrupt near-surface ^{14}C dating (Goslar et al., 2005). Given such chronological limitations, we refrained from making conclusions on recent peatland vegetation trends at sub-centennial timescales. However, at the broad ~200-year resolution of our analyses, we identified similar, recent shifts to high *Sphagnum* abundance in well-dated cores from regions of discontinuous and sporadic permafrost. For example, several cores from Fennoscandia (Sim et al., 2021) and the Seward Peninsula, Alaska (Hunt et al., 2013) exhibited increased *Sphagnum* abundance after ~400 years BP in response to 20th century climate warming and late-Holocene permafrost aggradation and thaw.

4.2. The importance of peatland hydrology for shrubification

Our catalogue of plant macrofossil records provides further evidence that Holocene tree and shrub growth on circum-Arctic peatlands has predominantly coincided with shifts to raised and drier peatland surfaces, resulting from autogenic peat accumulation, warming climates, and peat permafrost aggradation. However, recent shrubification signals were often concealed in non-normalised trendlines, because increases to binned relative abundances of woody vegetation were comparatively smaller during recent centuries than increases to *Sphagnum* (Figs. S1–3), which accelerated following late-Holocene FBTs and peat permafrost expansion. Woody vegetation and *Sphagnum* showed strong dissimilarity to wet-favouring herbaceous taxa (Fig. 5) and both PFTs expanded through time as herbaceous vegetation declined (Fig. 2). Herbaceous species presently dominate water-saturated fens and thermokarst wetlands (Vitt, 2006; Treat et al., 2016), with high water tables and anoxic conditions that restrict shrub and tree root growth (Szumigalski and Bayley, 1996; Jones et al., 2013). Our findings generally concur with recent experimental studies that have shown increased seedling survival on raised *Sphagnum* hummocks (Holmgren et al., 2015) and that increased evapotranspiration from newly-established trees may provide a positive feedback that further encourages woody encroachment (Limpens et al., 2014a). However, woody decline was also identified

in several palsas/peat plateaus and bogs experiencing rapid, recent *Sphagnum* expansion (van Bellen et al., 2011; Tremblay et al., 2014; Magnan et al., 2018; Sim et al., 2021), suggesting that *Sphagnum* can sometimes outcompete ligneous species through rapid vertical growth (Ohlson et al., 2001) or by engineering conditions that are slowly-draining, acidic, and nutrient-poor (van Breemen, 1995). While our study sought to establish between-site trends in past peatland vegetation change across the circum-Arctic, future studies could further investigate the importance of local hydrology and peatland microhabitat on the within-site variability of vegetation succession through analyses of closely-sampled, replicate cores (e.g., Piilo et al., 2022).

We found limited evidence of woody-herbaceous communities developing during recent centuries, although this may partly reflect a sampling bias in existing palaeoecological studies towards *Sphagnum*-dominated microhabitats, and shrubified fens presently exist in some boreal permafrost regions (e.g., Davies et al. (2022)). Future palaeoecological analyses of cores from such fen sites may reveal alternative mechanisms for recent peatland shrubification. During the mid- and late-Holocene, woody vegetation developed in some herbaceous-dominated cores in eastern Canada, prior to major *Sphagnum* establishment (Loisel and Garneau, 2010; Tremblay et al., 2014; Primeau and Garneau, 2021; Robitaille et al., 2021) (Figs. 3 and S2). Climate drying may have facilitated this temporary shrubification of fens by deepening water tables (Loisel and Garneau, 2010; Robitaille et al., 2021), because abundances of woody vegetation subsequently declined as regional precipitation increased in Quebec and Labrador after ~5000 years BP (Viau and Gajewski, 2009). Available peatland water-table depth reconstructions, for example using testate amoebae, from boreal and coastal peatlands in eastern Canada indicate increased hydrological variability in the region from ~3000 years BP (van Bellen et al., 2011; Magnan and Garneau, 2014; Primeau and Garneau, 2021). However, similar palaeohydrological reconstructions have currently only been synthesised since the LIA for permafrost regions (Zhang et al., 2022), which prevented detailed comparisons with our findings. The development of additional, long-term palaeohydrological records for circum-Arctic peatlands would further elucidate the relative importance of water tables and climate for past peatland shrubification.

The widespread Holocene expansion of *Sphagnum* in our dataset is consistent with previous syntheses of northern peat core records (Treat et al., 2016; Treat and Jones, 2018; Magnan et al., 2022), but unravelling the implications of the shift to *Sphagnum*-dominated assemblages was complicated by an absence of species-level records for more than a quarter of our compiled cores. *Sphagnum* mosses occupy wide environmental gradients, from minerotrophic, poor fens (e.g., *S. riparium* and *S. lindbergii*) to ombrotrophic bogs (e.g., *S. fuscum*, *S. rubellum* or *S. capillifolium*) (Treat and Jones, 2018; Magnan et al., 2022). Relative abundance data at a species-level is therefore required to determine wetland types from plant macrofossil records (Treat et al., 2016). It may also be possible to infer environmental niches of Holocene *Sphagnum* communities through correlations with other PFTs, but the closed compositional nature of our dataset made such analyses unsuitable. Where species-level *Sphagnum* data were available, we found that *Sphagnum* expansion in the vast majority of cases was associated with eventual shifts to ombrotrophic indicators ($n = 31$ cores), while only three cores transitioned towards hydrophilic *Sphagnum*. However, this finding should be interpreted cautiously, and we reinforce previous recommendations that future studies should differentiate between *Sphagnum* species to improve palaeoecological reconstructions.

Our long-term palaeoecological analyses suggest that future peatland shrubification may occur heterogeneously in circum-Arctic peatlands under 21st century warming, and will likely be limited to sites where dry, ombrotrophic microhabitats persist. Warming climates can shift the hydrological balance of permafrost peatlands in divergent trajectories, as shown by recent palaeohydrological studies of changing peatland surface wetness since the LIA (Sim et al., 2021; Zhang et al., 2022), with important implications for peatland vegetation composition. Projected future warming is expected to cause widespread peat permafrost degradation (Fewster et al., 2022) and peatland inundation (Olefeldt et al., 2016), but also increased surface drying through enhanced evapotranspiration (Swindles et al., 2015). Our Holocene dataset indicates that woody growth was initially restricted in sites that became saturated post-thaw, which resulted in rising abundances of sedges and hydrophilic *Sphagnum*. However, future plant productivity increases under warming climates could accelerate peat accumulation and FBTs, which previously drove increases to woody vegetation and *Sphagnum* sect. *Acutifolia* in the studied records. Furthermore, recent ice-wedge degradation has drained polygon depressions (Wolter et al., 2016), which may raise the likelihood of future shrub encroachment at northern high latitudes.

5. Conclusions

Our synthesis of plant macrofossil records from peatlands in the circum-Arctic permafrost region indicates a consistent, widespread expansion of woody vegetation and *Sphagnum* in circum-Arctic peatlands from ~8000 years BP to present, as herbaceous vegetation declined. Transitions from herbaceous vegetation to *Sphagnum* accelerated after ~1000 years BP, coinciding with continued neoglacial cooling and extensive peat permafrost aggradation. *Sphagnum* expanded rapidly after ~800 years BP in sites located in present-day regions of discontinuous and isolated permafrost, while non-*Sphagnum* mosses have become dominant in the continuous permafrost zone. Peatland shrubification during recent centuries was highly spatially variable, with our dataset evidencing widespread increases in Fennoscandia but a general decline in western and eastern Canada. Our findings suggest that shrub and tree growth will not occur as widely in circum-Arctic peatlands under 21st century climate warming as in upland tundra environments, and will more likely be restricted to peatlands experiencing surface drying.

Author contributions

Richard E. Fewster: Conceptualization, Methodology, Software, Formal analysis, Investigation, Resources, Data Curation, Writing - Original Draft, Writing - Review & Editing, Visualization, Project administration, Funding acquisition. **Paul J. Morris:** Conceptualization, Methodology, Supervision, Writing - Review & Editing, Project administration. **Graeme T. Swindles:** Conceptualization, Methodology, Supervision, Resources, Writing - Review & Editing. **Ruza F Ivanovic:** Supervision, Writing - Review & Editing. **Claire C. Treat:** Resources, Supervision, Writing - Review & Editing, Funding acquisition. **Miriam C. Jones:** Resources, Supervision, Writing - Review & Editing, Funding acquisition.

Declaration of competing interest

The authors declare that they have no known competing financial interests or personal relationships that could have appeared to influence the work reported in this paper.

Data availability

Data used to produce this research are included in the Supplementary Information and in Supplementary Datasets S1 and S2.

Acknowledgements

R.E.F. is in receipt of a UK Natural Environment Research Council Training Grant (no. NE/S007458/1). C.C.T. is supported by a European Research Council Horizon 2020 grant (no. 851181) and the Helmholtz Impulse and Networking Fund. M.C.J. is funded by the USGS Climate Research and Development Program.

Appendix A. Supplementary data

Supplementary data to this article can be found online at https://doi.org/10.1016/j.quascirev.2023.108055.

References

Aquino-López, M.A., Blaauw, M., Christen, J.A., Sanderson, N.K., 2018. Bayesian analysis of 210Pb dating. J. Agric. Biol. Environ. Stat. 23, 317–333. https://doi.org/10.1007/s13253-018-0328-7.

Bauer, I.E., Vitt, D.H., 2011. Peatland dynamics in a complex landscape: development of a fen-bog complex in the sporadic discontinuous permafrost zone of northern Alberta, Canada: development of peatland in the sporadic discontinuous permafrost zone, Canada. Boreas 40, 714–726. https://doi.org/10.1111/j.1502-3885.2011.00210.x.

Beaulieu-Audy, V., Garneau, M., Richard, P.J.H., Asnong, H., 2009. Holocene palaeoecological reconstruction of three boreal peatlands in the La Grande Rivière region, Québec, Canada. Holocene 19, 459–476. https://doi.org/10.1177/0959683608101395.

Belyea, L.R., 2009. Nonlinear dynamics of peatlands and potential feedbacks on the climate system. In: Carbon Cycling in Northern Peatlands. American Geophysical Union (AGU), pp. 5–18. https://doi.org/10.1029/2008GM000829.

Blaauw, M., 2010. Methods and code for 'classical' age-modelling of radiocarbon sequences. Quat. Geochronol. 5, 512–518. https://doi.org/10.1016/j.quageo.2010.01.002.

Blaauw, M., Christen, J.A., 2011. Flexible paleoclimate age-depth models using an autoregressive gamma process. Bayesian Anal 6, 457–474. https://doi.org/10.1214/11-BA618.

Brown, J., Ferrians, O., Heginbottom, J., Melnikov, E., 2002. Circum-Arctic Map of Permafrost and Ground-Ice Conditions. USA Natl. Snow Ice Data Cent, Boulder Colo version 2.

Camill, P., 1999. Peat accumulation and succession following permafrost thaw in the boreal peatlands of Manitoba, Canada. Ecoscience 6, 592–602. https://doi.org/10.1080/11956860.1999.11682561.

Camill, P., Barry, A., Williams, E., Andreassi, C., Limmer, J., Solick, D., 2009. Climate-vegetation-fire interactions and their impact on long-term carbon dynamics in a boreal peatland landscape in northern Manitoba, Canada. J. Geophys. Res. Biogeosciences 114. https://doi.org/10.1029/2009JG001071.

Camill, P., Lynch, J.A., Clark, J.S., Adams, J.B., Jordan, B., 2001. Changes in biomass, aboveground net primary production, and peat accumulation following permafrost thaw in the boreal peatlands of manitoba, Canada. Ecosystems 4, 461–478. https://doi.org/10.1007/s10021-001-0022-3.

Chen, Y., Hu, F.S., Lara, M.J., 2021. Divergent shrub-cover responses driven by climate, wildfire, and permafrost interactions in Arctic tundra ecosystems. Global Change Biol. 27, 652–663. https://doi.org/10.1111/gcb.15451.

Clarke, K.R., 1993. Non-parametric multivariate analyses of changes in community structure. Austral Ecol. 18, 117–143. https://doi.org/10.1111/j.1442-9993.1993.tb00438.x.

Davies, M.A., Mclaughlin, J.W., Packalen, M.S., Finkelstein, S.A., 2022. Holocene carbon storage and testate amoeba community structure in treed peatlands of the western Hudson Bay Lowlands margin, Canada. J. Quat. Sci. n/a. https://doi.org/10.1002/jqs.3465.

de Klerk, P., Donner, N., Karpov, N.S., Minke, M., Joosten, H., 2011. Short-term dynamics of a low-centred ice-wedge polygon near Chokurdakh (NE Yakutia, NE Siberia) and climate change during the last ca 1250 years. Quat. Sci. Rev. 30, 3013–3031.

Edvardsson, J., Stoffel, M., Corona, C., Bragazza, L., Leuschner, H.H., Charman, D.J., Helama, S., 2016. Subfossil peatland trees as proxies for Holocene palaeohydrology and palaeoclimate. Earth Sci. Rev. 163, 118–140. https://doi.org/10.1016/j.earscirev.2016.10.005.

Ellis, C.J., Rochefort, L., 2004. CENTURY-SCALE development of polygon-patterned tundra wetland, bylot island (73° N, 80° W). Ecology 85, 963–978. https://doi.org/10.1890/02-0614.

Fang, K., Morris, J.L., Salonen, J.S., Miller, P.A., Renssen, H., Sykes, M.T., Seppä, H., 2013. How robust are Holocene treeline simulations? A model–data comparison in the European Arctic treeline region. J. Quat. Sci. 28, 595–604. https://doi.org/10.1002/jqs.2654.

Fewster, R.E., Morris, P.J., Ivanovic, R.F., Swindles, G.T., Peregon, A.M., Smith, C.J., 2022. Imminent loss of climate space for permafrost peatlands in Europe and Western Siberia. Nat. Clim. Change 12, 373–379. https://doi.org/10.1038/s41558-022-01296-7.

Fewster, R.E., Morris, P.J., Swindles, G.T., Gregoire, L.J., Ivanovic, R.F., Valdes, P.J., Mullan, D., 2020. Drivers of Holocene palsa distribution in North America. Quat. Sci. Rev. 240, 106337. https://doi.org/10.1016/j.quascirev.2020.106337.

Fritz, M., Wolter, J., Rudaya, N., Palagushkina, O., Nazarova, L., Obu, J., Rethemeyer, J., Lantuit, H., Wetterich, S., 2016. Holocene ice-wedge polygon development in northern Yukon permafrost peatlands (Canada). Quat. Sci. Rev. 147, 279–297. https://doi.org/10.1016/j.quascirev.2016.02.008.

Gajewski, K., 2015. Quantitative reconstruction of Holocene temperatures across the Canadian arctic and Greenland. Global Planet. Change 128, 14–23. https://doi.org/10.1016/j.gloplacha.2015.02.003.

Gajewski, K., Viau, A., Sawada, M., Atkinson, D., Wilson, S., 2001. Sphagnum peatland distribution in North America and Eurasia during the past 21,000 years. Global Biogeochem. Cycles 15, 297–310. https://doi.org/10.1029/2000GB001286.

Gałka, M., Swindles, G.T., Szal, M., Fulweber, R., Feurdean, A., 2018. Response of plant communities to climate change during the late Holocene: palaeoecological insights from peatlands in the Alaskan Arctic. Ecol. Indicat. 85, 525–536.

Gibson, C.M., Chasmer, L.E., Thompson, D.K., Quinton, W.L., Flannigan, M.D., Olefeldt, D., 2018. Wildfire as a major driver of recent permafrost thaw in boreal peatlands. Nat. Commun. 9, 3041. https://doi.org/10.1038/s41467-018-05457-1.

Goslar, T., van der Knaap, W.O., Hicks, S., Andrič, M., Czernik, J., Goslar, E., Räsänen, S., Hyötylä, H., 2005. Radiocarbon dating of modern peat profiles: pre- and post-bomb ^{14}C variations in the construction of age-depth models. Radiocarbon 47, 115–134. https://doi.org/10.1017/S0033822200052243.

Halsey, L.A., Vitt, D.H., Zoltai, S.C., 1995. Disequilibrium response of permafrost in boreal continental western Canada to climate change. Clim. Change 30, 57–73. https://doi.org/10.1007/BF01093225.

Heffernan, L., Cavaco, M.A., Bhatia, M.P., Estop-Aragonés, C., Knorr, K.-H., Olefeldt, D., 2022. High peatland methane emissions following permafrost thaw: enhanced acetoclastic methanogenesis during early successional stages. Biogeosciences 19, 3051–3071. https://doi.org/10.5194/bg-19-3051-2022.

Heijmans, M.M.P.D., Magnússon, R., Lara, M., Frost, G., Myers-Smith, I., Van Huissteden, K., Jorgenson, M., Fedorov, A., Epstein, H., Lawrence, D., Limpens, J., 2022. Tundra vegetation change and impacts on permafrost. Nat. Rev. Earth Environ. 3, 68–84. https://doi.org/10.1038/s43017-021-00233-0.

Heijmans, M.M.P.D., van der Knaap, Y.A.M., Holmgren, M., Limpens, J., 2013. Persistent versus transient tree encroachment of temperate peat bogs: effects of climate warming and drought events. Global Change Biol. 19, 2240–2250. https://doi.org/10.1111/gcb.12202.

Helbig, M., Boike, J., Langer, M., Schreiber, P., Runkle, B.R.K., Kutzbach, L., 2013. Spatial and seasonal variability of polygonal tundra water balance: lena River Delta, northern Siberia (Russia). Hydrogeol. J. 21, 133–147. https://doi.org/10.1007/s10040-012-0933-4.

Hiller, A., Boettger, T., Kremenetski, C., 2001. Mediaeval climatic warming recorded by radiocarbon dated alpine tree-line shift on the Kola Peninsula, Russia. Holocene 11, 491–497. https://doi.org/10.1191/095968301678302931.

Holmes, M.E., Crill, P.M., Burnett, W.C., McCalley, C.K., Wilson, R.M., Frolking, S., Chang, K.-Y., Riley, W.J., Varner, R.K., Hodgkins, S.B., Coordinators, I.P., Team, I.F., McNichol, A.P., Saleska, S.R., Rich, V.I., Chanton, J.P., 2022. Carbon accumulation, flux, and fate in stordalen mire, a permafrost peatland in transition. Global Biogeochem. Cycles 36, e2021GB007113. https://doi.org/10.1029/2021GB007113.

Holmgren, M., Lin, C.-Y., Murillo, J.E., Nieuwenhuis, A., Penninkhof, J., Sanders, N., van Bart, T., van Veen, H., Vasander, H., Vollebregt, M.E., Limpens, J., 2015. Positive shrub–tree interactions facilitate woody encroachment in boreal peatlands. J. Ecol. 103, 58–66. https://doi.org/10.1111/1365-2745.12331.

Hugelius, G., Loisel, J., Chadburn, S., Jackson, R.B., Jones, M., MacDonald, G., Marushchak, M., Olefeldt, D., Packalen, M., Siewert, M.B., Treat, C., Turetsky, M., Voigt, C., Yu, Z., 2020. Large stocks of peatland carbon and nitrogen are vulnerable to permafrost thaw. Proc. Natl. Acad. Sci. USA 117, 20438–20446. https://doi.org/10.1073/pnas.1916387117.

Hunt, S., Yu, Z., Jones, M., 2013. Lateglacial and Holocene climate, disturbance and permafrost peatland dynamics on the Seward Peninsula, western Alaska. Quat. Sci. Rev. 63, 42–58. https://doi.org/10.1016/j.quascirev.2012.11.019.

Jones, M.C., Booth, R.K., Yu, Z., Ferry, P., 2013. A 2200-year record of permafrost dynamics and carbon cycling in a collapse-scar bog, interior Alaska. Ecosystems 16, 1–19. https://doi.org/10.1007/s10021-012-9592-5.

Jones, M.C., Harden, J., O'Donnell, J., Manies, K., Jorgenson, T., Treat, C., Ewing, S., 2017. Rapid carbon loss and slow recovery following permafrost thaw in boreal peatlands. Global Change Biol. 23, 1109–1127. https://doi.org/10.1111/gcb.13403.

Jones, M.C., Yu, Z., 2010. Rapid deglacial and early Holocene expansion of peatlands in Alaska. Proc. Natl. Acad. Sci. USA 107, 7347–7352. https://doi.org/10.1073/pnas.0911387107.

Kaufman, D.S., Ager, T.A., Anderson, N.J., Anderson, P.M., Andrews, J.T., Bartlein, P.J., Brubaker, L.B., Coats, L.L., Cwynar, L.C., Duvall, M.L., Dyke, A.S., Edwards, M.E., Eisner, W.R., Gajewski, K., Geirsdóttir, A., Hu, F.S., Jennings, A.E., Kaplan, M.R., Kerwin, M.W., Lozhkin, A.V., MacDonald, G.M., Miller, G.H., Mock, C.J., Oswald, W.W., Otto-Bliesner, B.L., Porinchu, D.F., Rühland, K., Smol, J.P., Steig, E.J., Wolfe, B.B., 2004. Holocene thermal maximum in the western Arctic (0–180°W). Quat. Sci. Rev. 23, 529–560. https://doi.org/10.1016/j.quascirev.2003.09.007.

Kaufman, D.S., Axford, Y.L., Henderson, A.C.G., McKay, N.P., Oswald, W.W., Saenger, C., Anderson, R.S., Bailey, H.L., Clegg, B., Gajewski, K., Hu, F.S., Jones, M.C., Massa, C., Routson, C.C., Werner, A., Wooller, M.J., Yu, Z., 2016. Holocene climate changes in eastern Beringia (NW North America) – a systematic review of multi-proxy evidence. Quat. Sci. Rev., Special Issue: PAST

Gateways (Palaeo-Arctic Spatial and Temporal Gateways) 147, 312–339. https://doi.org/10.1016/j.quascirev.2015.10.021.
Kettles, I.M., Robinson, S.D., Bastien, D.F., Garneau, M., Hall, G.E.M., 2003. PHYSICAL, GEOCHEMICAL, MACROFOSSIL and GROUND PENETRATING RADAR INFORMATION on FOURTEEN PERMAFROST-AFFECTED PEATLANDS IN the MACKENZIE VALLEY, NORTHWEST TERRITORIES (No. Open File 4007). Geological Sruvey of Canada.
Kjellman, S.E., Axelsson, P.E., Etzelmüller, B., Westermann, S., Sannel, A.B.K., 2018. Holocene development of subarctic permafrost peatlands in Finnmark, northern Norway. Holocene 28, 1855–1869. https://doi.org/10.1177/0959683618798126.
Korhola, A., Vasko, K., Toivonen, H., Olander, H., 2002. Holocene temperature changes in northern Fennoscandia reconstructed from chironomids using Bayesian modelling. Quat. Sci. Rev. 21, 1841–1860. https://doi.org/10.1016/S0277-3791(02)00003-3.
Kuhry, P., 2008. Palsa and peat plateau development in the Hudson Bay Lowlands, Canada: timing, pathways and causes. Boreas 37, 316–327.
Kullman, L., 2015. Higher-than-present medieval pine (Pinus sylvestris) treeline along the Swedish scandes. Landsc. https://doi.org/10.3097/LO.201542. Online 42–42.
Langlais, K., Bhiry, N., Lavoie, M., 2021. Holocene dynamics of an inland palsa peatland at Wiyâshâkimî Lake (Nunavik, Canada). Ecoscience 28, 269–282. https://doi.org/10.1080/11956860.2021.1907975.
Leuschner, H.H., Sass-Klaassen, U., Jansma, E., Baillie, M.G.L., Spurk, M., 2002. Subfossil European bog oaks: population dynamics and long-term growth depressions as indicators of changes in the Holocene hydro-regime and climate. Holocene 12, 695–706. https://doi.org/10.1191/0959683602hl584rp.
Limpens, J., Fijen, T.P.M., Keizer, I., Meijer, J., Olsthoorn, F., Pereira, A., Postma, R., Suyker, M., Vasander, H., Holmgren, M., 2021. Shrubs and degraded permafrost pave the way for tree establishment in subarctic peatlands. Ecosystems 24, 370–383. https://doi.org/10.1007/s10021-020-00523-6.
Limpens, J., Holmgren, M., Jacobs, C.M.J., , Zee, S.E.A.T.M.V. der, Karofeld, E., Berendse, F., 2014a. How does tree density affect water loss of peatlands? A mesocosm experiment. PLoS One 9, e91748. https://doi.org/10.1371/journal.pone.0091748.
Limpens, J., van Egmond, E., Li, B., Holmgren, M., 2014b. Do plant traits explain tree seedling survival in bogs? Funct. Ecol. 28, 283–290. https://doi.org/10.1111/1365-2435.12148.
Loisel, J., Bunsen, M., 2020. Abrupt fen-bog transition across southern patagonia: timing, causes, and impacts on carbon sequestration. Front. Ecol. Evol. 8.
Loisel, J., Gallego-Sala, A.V., Yu, Z., 2012. Global-scale pattern of peatland *Sphagnum* growth driven by photosynthetically active radiation and growing season length. Biogeosciences 9, 2737–2746. https://doi.org/10.5194/bg-9-2737-2012.
Loisel, J., Garneau, M., 2010. Late Holocene paleoecohydrology and carbon accumulation estimates from two boreal peat bogs in eastern Canada: potential and limits of multi-proxy archives. Palaeogeogr. Palaeoclimatol. Palaeoecol. 291, 493–533. https://doi.org/10.1016/j.palaeo.2010.03.020.
Loisel, J., Yu, Z., Beilman, D.W., Camill, P., Alm, J., Amesbury, M.J., Anderson, D., Andersson, S., Bochicchio, C., Barber, K., Belyea, L.R., Bunbury, J., Chambers, F.M., Charman, D.J., De Vleeschouwer, F., Fiałkiewicz-Kozieł, B., Finkelstein, S.A., Gałka, M., Garneau, M., Hammarlund, D., Hinchcliffe, W., Holmquist, J., Hughes, P., Jones, M.C., Klein, E.S., Kokfelt, U., Korhola, A., Kuhry, P., Lamarre, A., Lamentowicz, M., Large, D., Lavoie, M., MacDonald, G., Magnan, G., Mäkilä, M., Mallon, G., Mathijssen, P., Mauquoy, D., McCarroll, J., Moore, T.R., Nichols, J., O'Reilly, B., Oksanen, P., Packalen, M., Peteet, D., Richard, P.J., Robinson, S., Ronkainen, T., Rundgren, M., Sannel, A.B.K., Tarnocai, C., Thom, T., Tuittila, E.-S., Turetsky, M., Väliranta, M., van der Linden, M., van Geel, B., van Bellen, S., Vitt, D., Zhao, Y., Zhou, W., 2014. A database and synthesis of northern peatland soil properties and Holocene carbon and nitrogen accumulation. Holocene 24, 1028–1042. https://doi.org/10.1177/0959683614538073.
MacDonald, G.M., Beilman, D.W., Kremenetski, K.V., Sheng, Y., Smith, L.C., Velichko, A.A., 2006. Rapid early development of circumarctic peatlands and atmospheric CH_4 and CO_2 variations. Science 314, 285–288. https://doi.org/10.1126/science.1131722.
MacDonald, G.M., Velichko, A.A., Kremenetski, C.V., Borisova, O.K., Goleva, A.A., Andreev, A.A., Cwynar, L.C., Riding, R.T., Forman, S.L., Edwards, T.W.D., Aravena, R., Hammarlund, D., Szeicz, J.M., Gattaulin, V.N., 2000. Holocene treeline history and climate change across northern Eurasia. Quat. Res. 53, 302–311. https://doi.org/10.1006/qres.1999.2123.
Magnan, G., Garneau, M., 2014. Evaluating long-term regional climate variability in the maritime region of the St. Lawrence North Shore (eastern Canada) using a multi-site comparison of peat-based paleohydrological records. J. Quat. Sci. 29, 209–220. https://doi.org/10.1002/jqs.2694.
Magnan, G., Sanderson, N.K., Piilo, S., Pratte, S., Väliranta, M., van Bellen, S., Zhang, H., Garneau, M., 2022. Widespread recent ecosystem state shifts in high-latitude peatlands of northeastern Canada and implications for carbon sequestration. Global Change Biol. 28, 1919–1934. https://doi.org/10.1111/gcb.16032.
Magnan, G., van Bellen, S., Davies, L., Froese, D., Garneau, M., Mullan-Boudreau, G., Zaccone, C., Shotyk, W., 2018. Impact of the Little Ice Age cooling and 20th century climate change on peatland vegetation dynamics in central and northern Alberta using a multi-proxy approach and high-resolution peat chronologies. Quat. Sci. Rev. 185, 230–243. https://doi.org/10.1016/j.quascirev.2018.01.015.
Magnússon, R.Í., Limpens, J., Kleijn, D., van Huissteden, K., Maximov, T.C., Lobry, S., Heijmans, M.M.P.D., 2021. Shrub decline and expansion of wetland vegetation revealed by very high resolution land cover change detection in the Siberian lowland tundra. Sci. Total Environ. 782, 146877. https://doi.org/10.1016/j.scitotenv.2021.146877.
Mann, M.E., Zhang, Z., Rutherford, S., Bradley, R.S., Hughes, M.K., Shindell, D., Ammann, C., Faluvegi, G., Ni, F., 2009. Global signatures and dynamical origins of the Little ice age and medieval climate anomaly. Science 326, 1256–1260. https://doi.org/10.1126/science.1177303.
Mauquoy, D., Hughes, P.D.M., van Geel, B., 2010. A Protocol for Plant Macrofossil Analysis of Peat Deposits 6.
McKay, N.P., Kaufman, D.S., Routson, C.C., Erb, M.P., Zander, P.D., 2018. The onset and rate of Holocene neoglacial cooling in the arctic. Geophys. Res. Lett. 45 (12), 487. https://doi.org/10.1029/2018GL079773.
Mekonnen, Z.A., Riley, W.J., Berner, L.T., Bouskill, N.J., Torn, M.S., Iwahana, G., Breen, A.L., Myers-Smith, I.H., Criado, M.G., Liu, Y., Euskirchen, E.S., Goetz, S.J., Mack, M.C., Grant, R.F., 2021. Arctic tundra shrubification: a review of mechanisms and impacts on ecosystem carbon balance. Environ. Res. Lett. 16, 053001. https://doi.org/10.1088/1748-9326/abf28b.
Minke, M., Donner, N., Karpov, N., de Klerk, P., Joosten, H., 2009. Patterns in vegetation composition, surface height and thaw depth in polygon mires in the Yakutian Arctic (NE Siberia): a microtopographical characterisation of the active layer. Permafr. Periglac. Process. 20, 357–368. https://doi.org/10.1002/ppp.663.
Minke, M., Donner, N., Karpov, N., de Klerk, P., Joosten, H., 2007. Distribution, diversity, development and dynamics of polygon mires: examples from NE Yakutia (NE Siberia). Peatl. Int. 36–40.
Moore, T.R., Bubier, J.L., Bledzki, L., 2007. Litter decomposition in temperate peatland ecosystems: the effect of substrate and site. Ecosystems 10, 949–963.
Morris, P.J., Swindles, G.T., Valdes, P.J., Ivanovic, R.F., Gregoire, L.J., Smith, M.W., Tarasov, L., Haywood, A.M., Bacon, K.L., 2018. Global peatland initiation driven by regionally asynchronous warming. Proc. Natl. Acad. Sci. USA 115, 4851–4856. https://doi.org/10.1073/pnas.1717838115.
Myers-Smith, I.H., Elmendorf, S.C., Beck, P.S.A., Wilmking, M., Hallinger, M., Blok, D., Tape, K.D., Rayback, S.A., Macias-Fauria, M., Forbes, B.C., Speed, J.D.M., Boulanger-Lapointe, N., Rixen, C., Lévesque, E., Schmidt, N.M., Baittinger, C., Trant, A.J., Hermanutz, L., Collier, L.S., Dawes, M.A., Lantz, T.C., Weijers, S., Jørgensen, R.H., Buchwal, A., Buras, A., Naito, A.T., Ravolainen, V., Schaepman-Strub, G., Wheeler, J.A., Wipf, S., Guay, K.C., Hik, D.S., Vellend, M., 2015. Climate sensitivity of shrub growth across the tundra biome. Nat. Clim. Change 5, 887–891. https://doi.org/10.1038/nclimate2697.
Myers-Smith, I.H., Hik, D.S., 2018. Climate warming as a driver of tundra shrubline advance. J. Ecol. 106, 547–560. https://doi.org/10.1111/1365-2745.12817.
Nakatsubo, T., Uchida, M., Sasaki, A., Kondo, M., Yoshitake, S., Kanda, H., 2015. Carbon accumulation rate of peatland in the High Arctic, Svalbard: implications for carbon sequestration. Pol. Sci. 9, 267–275. https://doi.org/10.1016/j.polar.2014.12.002.
Ohlson, M., Økland, R.H., Nordbakken, J.-F., Dahlberg, B., 2001. Fatal interactions between Scots pine and Sphagnum mosses in bog ecosystems. Oikos 94, 425–432. https://doi.org/10.1034/j.1600-0706.2001.940305.x.
Oksanen, J., Simpson, G.L., Blanchet, F.G., Kindt, R., Legendre, P., Minchin, P.R., O'Hara, R.B., Solymos, P., Stevens, M.H.H., Szoecs, E., Wagner, H., Barbour, M., Bedward, M., Bolker, B., Borcard, D., Carvalho, G., Chirico, M., Caceres, M.D., Durand, S., Evangelista, H.B.A., FitzJohn, R., Friendly, M., Furneaux, B., Hannigan, G., Hill, M.O., Lahti, L., McGlinn, D., Ouellette, M.-H., Cunha, E.R., Smith, T., Stier, A., Braak, C.J.F.T., Weedon, J., 2022. Vegan: Community Ecology Package.
Oksanen, P.O., Kuhry, P., Alekseeva, R.N., 2003. Holocene development and permafrost history of the usinsk mire, northeast European Russia. Géogr. Phys. Quaternaire 57, 169–187. https://doi.org/10.7202/011312ar.
Oksanen, P.O., Kuhry, P., Alekseeva, R.N., 2001. Holocene development of the rogovaya river peat plateau, European Russian arctic. Holocene 11, 25–40. https://doi.org/10.1191/095968301675477157.
Olefeldt, D., Goswami, S., Grosse, G., Hayes, D., Hugelius, G., Kuhry, P., McGuire, A.D., Romanovsky, V.E., Sannel, A.B.K., Schuur, E.a.G., Turetsky, M.R., 2016. Circumpolar distribution and carbon storage of thermokarst landscapes. Nat. Commun. 7, 13043. https://doi.org/10.1038/ncomms13043.
Olefeldt, D., Heffernan, L., Jones, M.C., Sannel, A.B.K., Treat, C.C., Turetsky, M.R., 2021. Permafrost thaw in northern peatlands: rapid changes in ecosystem and landscape functions. In: Canadell, J.G., Jackson, R.B. (Eds.), Ecosystem Collapse and Climate Change, Ecological Studies. Springer International Publishing, Cham, pp. 27–67. https://doi.org/10.1007/978-3-030-71330-0_3.
Ouzilleau Samson, D., Bhiry, N., Lavoie, M., 2010. Late-Holocene palaeoecology of a polygonal peatland on the south shore of Hudson Strait, northern Québec, Canada. Holocene 20, 525–536.
Payette, S., 1984. Peat inception and climatic change in northern Quebec. In: Mörner, N.-A., Karlén, W. (Eds.), Climatic Changes on a Yearly to Millennial Basis: Geological, Historical and Instrumental Records. Springer Netherlands, Dordrecht, pp. 173–179. https://doi.org/10.1007/978-94-015-7692-5_17.
Payette, S., Lavoie, C., 1994. The arctic tree line as a record of past and recent climatic changes. Environ. Rev. 2, 78–90.
Pelletier, N., Talbot, J., Olefeldt, D., Turetsky, M., Blodau, C., Sonnentag, O., Quinton, W.L., 2017. Influence of Holocene permafrost aggradation and thaw on the paleoecology and carbon storage of a peatland complex in northwestern Canada. Holocene 27, 1391–1405. https://doi.org/10.1177/0959683617693899.
Peregon, A., Maksyutov, S., Kosykh, N.P., Mironycheva-Tokareva, N.P., 2008. Map-based inventory of wetland biomass and net primary production in western

Siberia. J. Geophys. Res. Biogeosciences 113. https://doi.org/10.1029/2007JG000441.
Piilo, S.R., Väliranta, M.M., Amesbury, M.J., Aquino-López, M.A., Charman, D.J., Gallego-Sala, A., Garneau, M., Koroleva, N., Kärppä, M., Laine, A.M., Sannel, A.B.K., Tuittila, E.-S., Zhang, H., 2022. Consistent centennial-scale change in European sub-Arctic peatland vegetation toward Sphagnum dominance—implications for carbon sink capacity. Glob. Change Biol. n/a. https://doi.org/10.1111/gcb.16554.
Pouliot, R., Rochefort, L., Karofeld, E., Mercier, C., 2011. Initiation of Sphagnum moss hummocks in bogs and the presence of vascular plants: is there a link? Acta Oecol. 37, 346–354. https://doi.org/10.1016/j.actao.2011.04.001.
Primeau, G., Garneau, M., 2021. Carbon accumulation in peatlands along a boreal to subarctic transect in eastern Canada. Holocene 31, 858–869. https://doi.org/10.1177/0959683620988031.
R Core Team, 2022. R: the R Project for Statistical Computing [WWW Document]. URL.
Reimer, P.J., Austin, W.E.N., Bard, E., Bayliss, A., Blackwell, P.G., Ramsey, C.B., Butzin, M., Cheng, H., Edwards, R.L., Friedrich, M., Grootes, P.M., Guilderson, T.P., Hajdas, I., Heaton, T.J., Hogg, A.G., Hughen, K.A., Kromer, B., Manning, S.W., Muscheler, R., Palmer, J.G., Pearson, C., Plicht, J. van der, Reimer, R.W., Richards, D.A., Scott, E.M., Southon, J.R., Turney, C.S.M., Wacker, L., Adolphi, F., Büntgen, U., Capano, M., Fahrni, S.M., Fogtmann-Schulz, A., Friedrich, R., Köhler, P., Kudsk, S., Miyake, F., Olsen, J., Reinig, F., Sakamoto, M., Sookdeo, A., Talamo, S., 2020. The IntCal20 northern hemisphere radiocarbon age calibration curve (0–55 cal kBP). Radiocarbon 62, 725–757. https://doi.org/10.1017/RDC.2020.41.
Robitaille, M., Garneau, M., van Bellen, S., Sanderson, N.K., 2021. Long-term and recent ecohydrological dynamics of patterned peatlands in north-central Quebec (Canada). Holocene 31, 844–857. https://doi.org/10.1177/0959683620988051.
Rodysill, J.R., Anderson, Lesleigh, Cronin, T.M., Jones, M.C., Thompson, R.S., Wahl, D.B., Willard, D.A., Addison, J.A., Alder, J.R., Anderson, K.H., Anderson, Lysanna, Barron, J.A., Bernhardt, C.E., Hostetler, S.W., Kehrwald, N.M., Khan, N.S., Richey, J.N., Starratt, S.W., Strickland, L.E., Toomey, M.R., Treat, C.C., Wingard, G.L., 2018. A north American hydroclimate synthesis (NAHS) of the common era. Global Planet. Change 162, 175–198. https://doi.org/10.1016/j.gloplacha.2017.12.025.
Rohatgi, A. 2021. WebPlotDigitizer (v.4.5). [Software] Available from: https://automeris.io/WebPlotDigitizer.
Salonen, J.S., Seppä, H., Väliranta, M., Jones, V.J., Self, A., Heikkilä, M., Kultti, S., Yang, H., 2011. The Holocene thermal maximum and late-Holocene cooling in the tundra of NE European Russia. Quat. Res. 75, 501–511. https://doi.org/10.1016/j.yqres.2011.01.007.
Sannel, A.B.K., Hempel, L., Kessler, A., Prskienis, V., 2018. Holocene development and permafrost history in sub-arctic peatlands in Tavvavuoma, northern Sweden. Boreas 47, 454–468. https://doi.org/10.1111/bor.12276.
Sannel, A.B.K., Kuhry, P., 2008. Long-term stability of permafrost in subarctic peat plateaus, west-central Canada. Holocene 18, 589–601. https://doi.org/10.1177/0959683608089658.
Sejrup, H.P., Seppä, H., McKay, N.P., Kaufman, D.S., Geirsdóttir, Á., de Vernal, A., Renssen, H., Husum, K., Jennings, A., Andrews, J.T., 2016. North Atlantic-Fennoscandian Holocene climate trends and mechanisms. Quat. Sci. Rev., Special Issue: PAST Gateways (Palaeo-Arctic Spatial and Temporal Gateways) 147, 365–378. https://doi.org/10.1016/j.quascirev.2016.06.005.
Seppä, H., Birks, H.J.B., 2001. July Mean temperature and annual precipitation trends during the Holocene in the Fennoscandian tree-line area: pollen-based climate reconstructions. Holocene 11, 527–539. https://doi.org/10.1191/095968301680223486.
Sim, T.G., Swindles, G.T., Morris, P., Gałka, M., Mullan, D., Galloway, J., 2019. Pathways for ecological change in Canadian High Arctic wetlands under rapid twentieth century warming. Geophys. Res. Lett. 46, 4726–4737.
Sim, T.G., Swindles, G.T., Morris, P.J., Baird, A.J., Cooper, C.L., Gallego-Sala, A.V., Charman, D.J., Roland, T.P., Borken, W., Mullan, D.J., 2021. Divergent responses of permafrost peatlands to recent climate change. Environ. Res. Lett. 16, 034001.
Swindles, G.T., Morris, P.J., Mullan, D., Watson, E.J., Turner, T.E., Roland, T.P., Amesbury, M.J., Kokfelt, U., Schoning, K., Pratte, S., Gallego-Sala, A., Charman, D.J., Sanderson, N., Garneau, M., Carrivick, J.L., Woulds, C., Holden, J., Parry, L., Galloway, J.M., 2015. The long-term fate of permafrost peatlands under rapid climate warming. Sci. Rep. 5, 17951. https://doi.org/10.1038/srep17951.
Szumigalski, A.R., Bayley, S.E., 1996. Net above-ground primary production along a bog-rich fen gradient in Central Alberta, Canada. Wetlands 16, 467–476. https://doi.org/10.1007/BF03161336.
Teltewskoi, A., Beermann, F., Beil, I., Bobrov, A., De Klerk, P., Lorenz, S., Lüder, A., Michaelis, D., Joosten, H., 2016. 4000 years of changing wetness in a permafrost polygon peatland (Kytalyk, NE Siberia): a comparative high-resolution multi-proxy study. Permafr. Periglac. Process. 27, 76–95.
Treat, C.C., Jones, M.C., 2018. Near-surface permafrost aggradation in Northern Hemisphere peatlands shows regional and global trends during the past 6000 years. Holocene 28, 998–1010. https://doi.org/10.1177/0959683617752858.
Treat, C.C., Jones, M.C., Brosius, L., Grosse, G., Walter Anthony, K., Frolking, S., 2021. The role of wetland expansion and successional processes in methane emissions from northern wetlands during the Holocene. Quat. Sci. Rev. 257, 106864. https://doi.org/10.1016/j.quascirev.2021.106864.
Treat, C.C., Jones, M.C., Camill, P., Gallego-Sala, A., Garneau, M., Harden, J.W., Hugelius, G., Klein, E.S., Kokfelt, U., Kuhry, P., Loisel, J., Mathijssen, P.J.H., O'Donnell, J.A., Oksanen, P.O., Ronkainen, T.M., Sannel, A.B.K., Talbot, J., Tarnocai, C., Väliranta, M., 2016. Effects of permafrost aggradation on peat properties as determined from a pan-Arctic synthesis of plant macrofossils. J. Geophys. Res. Biogeosciences 121, 78–94. https://doi.org/10.1002/2015JG003061.
Tremblay, S., Bhiry, N., Lavoie, M., 2014. Long-term dynamics of a palsa in the sporadic permafrost zone of northwestern Quebec (Canada). Can. J. Earth Sci. 51, 500–509. https://doi.org/10.1139/cjes-2013-0123.
Turetsky, M.R., Benscoter, B., Page, S., Rein, G., van der Werf, G.R., Watts, A., 2015. Global vulnerability of peatlands to fire and carbon loss. Nat. Geosci. 8, 11–14. https://doi.org/10.1038/ngeo2325.
Ullman, D.J., Carlson, A.E., Hostetler, S.W., Clark, P.U., Cuzzone, J., Milne, G.A., Winsor, K., Caffee, M., 2016. Final Laurentide ice-sheet deglaciation and Holocene climate-sea level change. Quat. Sci. Rev. 152, 49–59. https://doi.org/10.1016/j.quascirev.2016.09.014.
Väliranta, M., Kaakinen, A., Kuhry, P., 2003. Holocene climate and landscape evolution east of the pechora delta, east-European Russian arctic. Quat. Res. 59, 335–344. https://doi.org/10.1016/S0033-5894(03)00041-3.
Väliranta, M., Marushchak, M.E., Tuovinen, J.-P., Lohila, A., Biasi, C., Voigt, C., Zhang, H., Piilo, S., Virtanen, T., Räsänen, A., Kaverin, D., Pastukhov, A., Sannel, A.B.K., Tuittila, E.-S., Korhola, A., Martikainen, P.J., 2021. Warming climate forcing impact from a sub-arctic peatland as a result of late Holocene permafrost aggradation and initiation of bare peat surfaces. Quat. Sci. Rev. 264, 107022. https://doi.org/10.1016/j.quascirev.2021.107022.
Väliranta, M., Salojärvi, N., Vuorsalo, A., Juutinen, S., Korhola, A., Luoto, M., Tuittila, E.-S., 2017. Holocene fen–bog transitions, current status in Finland and future perspectives. Holocene 27, 752–764. https://doi.org/10.1177/0959683616670471.
Van Bellen, S., Garneau, M., Ali, A.A., Lamarre, A., Robert, É.C., Magnan, G., Asnong, H., Pratte, S., 2013. Poor fen succession over ombrotrophic peat related to late Holocene increased surface wetness in subarctic Quebec, Canada. J. Quat. Sci. 28, 748–760. https://doi.org/10.1002/jqs.2670.
van Bellen, S., Garneau, M., Booth, R.K., 2011. Holocene carbon accumulation rates from three ombrotrophic peatlands in boreal Quebec, Canada: impact of climate-driven ecohydrological change. Holocene 21, 1217–1231. https://doi.org/10.1177/0959683611405243.
van Breemen, N., 1995. How Sphagnum bogs down other plants. Trends Ecol. Evol. 10, 270–275. https://doi.org/10.1016/0169-5347(95)90007-1.
Vardy, S.R., Warner, B.G., Aravena, R., 1998. Holocene climate and the development of a subarctic peatland near inuvik, northwest territories, Canada. Clim. Change 40, 285–313. https://doi.org/10.1023/A:1005473021115.
Vardy, S.R., Warner, B.G., Aravena, R., 1997. Holocene climate effects on the development of a peatland on the tuktoyaktuk Peninsula, northwest Territories1. Quat. Res. 47, 90–104. https://doi.org/10.1006/qres.1996.1869.
Vardy, S.R., Warner, B.G., Asada, T., 2005. Holocene environmental change in two polygonal peatlands, south-central Nunavut, Canada. Boreas 34, 324–334.
Varner, R.K., Crill, P.M., Frolking, S., McCalley, C.K., Burke, S.A., Chanton, J.P., Holmes, M.E., , Isogenie Project Coordinators, Saleska, S., Palace, M.W., 2022. Permafrost thaw driven changes in hydrology and vegetation cover increase trace gas emissions and climate forcing in Stordalen Mire from 1970 to 2014. Philos. Trans. R. Soc. Math. Phys. Eng. Sci. 380, 20210022. https://doi.org/10.1098/rsta.2021.0022.
Viau, A.E., Gajewski, K., 2009. Reconstructing millennial-scale, regional paleoclimates of boreal Canada during the Holocene. J. Clim. 22, 316–330.
Vicherová, E., Hájek, M., Hájek, T., 2015. Calcium intolerance of fen mosses: physiological evidence, effects of nutrient availability and successional drivers. Perspect. Plant Ecol. Evol. Systemat. 17, 347–359. https://doi.org/10.1016/j.ppees.2015.06.005.
Vitt, D.H., 2006. Functional characteristics and indicators of boreal peatlands. In: Wieder, R.K., Vitt, D.H. (Eds.), Boreal Peatland Ecosystems, Ecological Studies. Springer, Berlin, Heidelberg, pp. 9–24. https://doi.org/10.1007/978-3-540-31913-9_2.
Walker, M., Head, M.J., Lowe, J., Berkelhammer, M., BjÖrck, S., Cheng, H., Cwynar, L.C., Fisher, D., Gkinis, V., Long, A., Newnham, R., Rasmussen, S.O., Weiss, H., 2019. Subdividing the Holocene Series/Epoch: formalization of stages/ages and subseries/subepochs, and designation of GSSPs and auxiliary stratotypes. J. Quat. Sci. 34, 173–186. https://doi.org/10.1002/jqs.3097.
Weckström, J., Seppä, H., Korhola, A., 2010. Climatic influence on peatland formation and lateral expansion in sub-arctic Fennoscandia. Boreas 39, 761–769. https://doi.org/10.1111/j.1502-3885.2010.00168.x.
Werner, J.P., Divine, D.V., Charpentier Ljungqvist, F., Nilsen, T., Francus, P., 2018. Spatio-temporal variability of Arctic summer temperatures over the past 2 millennia. Clim. Past 14, 527–557. https://doi.org/10.5194/cp-14-527-2018.
Wolter, J., Lantuit, H., Fritz, M., Macias-Fauria, M., Myers-Smith, I., Herzschuh, U., 2016. Vegetation composition and shrub extent on the Yukon coast, Canada, are strongly linked to ice-wedge polygon degradation. Polar Res. 35, 27489. https://doi.org/10.3402/polar.v35.27489.
Woo, M., Young, K.L., 2006. High Arctic wetlands: their occurrence, hydrological characteristics and sustainability. J. Hydrol., Groundwater - surface water interactions in wetlands for integrated water resources management 320, 432–450. https://doi.org/10.1016/j.jhydrol.2005.07.025.
Yu, Z., Loisel, J., Brosseau, D.P., Beilman, D.W., Hunt, S.J., 2010. Global peatland dynamics since the last glacial maximum. Geophys. Res. Lett. 37. https://doi.org/10.1029/2010GL043584.
Zhang, H., Amesbury, M.J., Piilo, S.R., Garneau, M., Gallego-Sala, A., Väliranta, M.M., 2020. Recent changes in peatland testate amoeba functional traits and

hydrology within a replicated site network in northwestern québec, Canada. Front. Ecol. Evol. 8.

Zhang, H., Piilo, S.R., Amesbury, M.J., Charman, D.J., Gallego-Sala, A.V., Väliranta, M.M., 2018. The role of climate change in regulating Arctic permafrost peatland hydrological and vegetation change over the last millennium. Quat. Sci. Rev. 182, 121–130. https://doi.org/10.1016/j.quascirev.2018.01.003.

Zhang, H., Väliranta, M., Swindles, G.T., Aquino-López, M.A., Mullan, D., Tan, N., Amesbury, M., Babeshko, K.V., Bao, K., Bobrov, A., Chernyshov, V., Davies, M.A., Diaconu, A.-C., Feurdean, A., Finkelstein, S.A., Garneau, M., Guo, Z., Jones, M.C., Kay, M., Klein, E.S., Lamentowicz, M., Magnan, G., Marcisz, K., Mazei, N., Mazei, Y., Payne, R., Pelletier, N., Piilo, S.R., Pratte, S., Roland, T., Saldaev, D., Shotyk, W., Sim, T.G., Sloan, T.J., Słowiński, M., Talbot, J., Taylor, L., Tsyganov, A.N., Wetterich, S., Xing, W., Zhao, Y., 2022. Recent climate change has driven divergent hydrological shifts in high-latitude peatlands. Nat. Commun. 13, 4959. https://doi.org/10.1038/s41467-022-32711-4.

Zoltai, S.C., 1993. Cyclic development of permafrost in the peatlands of northwestern Alberta, Canada. Arct. Alp. Res. 25, 240. https://doi.org/10.2307/1551820.

Zoltai, S.C., Tarnocai, C., 1975. Perennially frozen peatlands in the western arctic and subarctic of Canada. Can. J. Earth Sci. 12, 28–43. https://doi.org/10.1139/e75-004.